2. Arvanitakis Z, Wilson RS, Bienias JL, Evans DA, Bennett DA. Diabetes mellitus and risk of Alzheimer disease and decline in cognitive function. Arch Neurol 2004;61:661–666.
3. Gregg EW, Yaffe K, Cauley JA, et al. Is diabetes associated with cognitive impairment and cognitive decline among older women? Study of Osteoporotic Fractures Research Group. Arch Intern Med 2000;160:174–180.
4. Ott A, Stolk RP, van Harskamp F, Pols HA, Hofman A, Breteler MM. Diabetes mellitus and the risk of dementia: The Rotterdam Study. Neurology 1999;53:1937–1942.
5. Peila R, Rodriguez BL, Launer LJ. Type 2 diabetes, APOE gene, and the risk for dementia and related pathologies: The Honolulu-Asia Aging Study. Diabetes 2002;51:1256–1262.
6. MacKnight C, Rockwood K, Awalt E, McDowell I. Diabetes mellitus and the risk of dementia, Alzheimer's disease and vascular cognitive impairment in the Canadian Study of Health and Aging. Dement Geriatr Cogn Disord 2002; 14:77–83.
7. Schnaider Beeri M, Goldbourt U, Silverman JM, et al. Diabetes mellitus in midlife and the risk of dementia three decades later. Neurology 2004;63:1902–1907.
8. Haan MN. Therapy insight: type 2 diabetes mellitus and the risk of late-onset Alzheimer's disease. Nat Clin Pract Neurol 2006;2:159–166.
9. Yoshitake T, Kiyohara Y, Kato I, et al. Incidence and risk factors of vascular dementia and Alzheimer's disease in a defined elderly Japanese population: the Hisayama Study. Neurology 1995;45:1161–1168.
10. Kuusisto J, Koivisto K, Mykkanen L, et al. Association between features of the insulin resistance syndrome and Alzheimer's disease independently of apolipoprotein E4 phenotype: cross sectional population based study. BMJ 1997;315:1045–1049.
11. Razay G, Wilcock GK. Hyperinsulinaemia and Alzheimer's disease. Age Ageing 1994;23:396–399.
12. Stolk RP, Breteler MM, Ott A, et al. Insulin and cognitive function in an elderly population: The Rotterdam Study. Diabetes Care 1997;20:792–795.
13. Peila R, Rodriguez BL, White LR, Launer LJ. Fasting insulin and incident dementia in an elderly population of Japanese-American men. Neurology 2004;63:228–233.
14. Luchsinger JA, Tang MX, Shea S, Mayeux R. Hyperinsulinemia and risk of Alzheimer disease. Neurology 2004;63: 1187–1192.
15. Whitmer RA. Type 2 diabetes and risk of cognitive impairment and dementia. Curr Neurol Neurosci Rep 2007;7: 373–380.
16. Stozicka Z, Zilka N, Novak M. Risk and protective factors for sporadic Alzheimer's disease. Acta Virol 2007;51:205–222.
17. Katsuki S. Epidemiological and clinicopathological study on cerebrovascular disease in Japan. Prog Brain Res 1966; 21:64–89.
18. Fujimi K, Sasaki K, Noda K, et al. Clinicopathological outline of dementia with Lewy bodies applying the revised criteria: the Hisayama Study. Brain Pathol 2008;18:317–325.
19. Ohmura T, Ueda K, Kiyohara Y, et al. Prevalence of type 2 (non-insulin-dependent) diabetes mellitus and impaired glucose tolerance in the Japanese general population: the Hisayama Study. Diabetologia 1993;36:1198–1203.
20. Matthews DR, Hosker JP, Rudenski AS, Naylor BA, Treacher DF, Turner RC. Homeostasis model assessment: insulin resistance and beta-cell function from fasting plasma glucose and insulin concentrations in man. Diabetologia 1985;28:412–419.
21. Mirra SS, Heyman A, McKeel D, et al. The Consortium to Establish a Registry for Alzheimer's Disease (CERAD): part II: standardization of the neuropathologic assessment of Alzheimer's disease. Neurology 1991;41:479–486.
22. Braak H, Alafuzoff I, Arzberger T, Kretzschmar H, Del Tredici K. Staging of Alzheimer disease-associated neurofibrillary pathology using paraffin sections and immunocytochemistry. Acta Neuropathol 2006;112:389–404.
23. Braak H, Braak E. Neuropathological stageing of Alzheimer-related changes. Acta Neuropathol 1991;82: 239–259.
24. Hardy J. Alzheimer's disease: the amyloid cascade hypothesis: an update and reappraisal. J Alzheimers Dis 2006;9: 151–153.
25. Frame S, Zheleva D. Targeting glycogen synthase kinase-3 in insulin signalling. Expert Opin Ther Targets 2006;10: 429–444.
26. Phiel CJ, Wilson CA, Lee VM, Klein PS. GSK-3α regulates production of Alzheimer's disease amyloid-β peptides. Nature 2003;423:435–439.
27. Kaytor MD, Orr HT. The GSK3β signaling cascade and neurodegenerative disease. Curr Opin Neurobiol 2002;12: 275–278.
28. Farris W, Mansourian S, Chang Y, et al. Insulin-degrading enzyme regulates the levels of insulin, amyloid β-protein, and the β-amyloid precursor protein intracellular domain in vivo. Proc Natl Acad Sci USA 2003;100:4162–4167.
29. Vekrellis K, Ye Z, Qiu WQ, et al. Neurons regulate extracellular levels of amyloid β-protein via proteolysis by insulin-degrading enzyme. J Neurosci 2000;20:1657–1665.
30. Gispen WH, Biessels GJ. Cognition and synaptic plasticity in diabetes mellitus. Trends Neurosci 2000;23:542–549.
31. Craft S, Asthana S, Cook DG, et al. Insulin dose-response effects on memory and plasma amyloid precursor protein in Alzheimer's disease: interactions with apolipoprotein E genotype. Psychoneuroendocrinology 2003;28:809–822.
32. Blass JP. Alzheimer's disease and Alzheimer's dementia: distinct but overlapping entities. Neurobiol Aging 2002; 23:1077–1084.
33. Heitner J, Dickson D. Diabetics do not have increased Alzheimer-type pathology compared with age-matched control subjects: a retrospective postmortem immunocytochemical and histofluorescent study. Neurology 1997;49: 1306–1311.
34. Beeri MS, Silverman JM, Davis KL, et al. Type 2 diabetes is negatively associated with Alzheimer's disease neuropathology. J Gerontol A Biol Sci Med Sci 2005;60:471–475.
35. Arvanitakis Z, Schneider JA, Wilson RS, et al. Diabetes is related to cerebral infarction but not to AD pathology in older persons. Neurology 2006;67:1960–1965.
36. Yang DS, Small DH, Seydel U, et al. Apolipoprotein E promotes the binding and uptake of β-amyloid into Chinese hamster ovary cells in an isoform-specific manner. Neuroscience 1999;90:1217–1226.
37. Namba Y, Tomonaga M, Kawasaki H, Otomo E, Ikeda K. Apolipoprotein E immunoreactivity in cerebral amyloid deposits and neurofibrillary tangles in Alzheimer's disease and kuru plaque amyloid in Creutzfeldt-Jakob disease. Brain Res 1991;541:163–166.
38. Dolev I, Michaelson DM. A nontransgenic mouse model shows inducible amyloid-β (Aβ) peptide deposition and elucidates the role of apolipoprotein E in the amyloid cascade. Proc Natl Acad Sci USA 2004;101: 13909–13914.

Mutation Research 703 (2010) 51–58

Contents lists available at ScienceDirect

Mutation Research/Genetic Toxicology and Environmental Mutagenesis

journal homepage: www.elsevier.com/locate/gentox
Community address: www.elsevier.com/locate/mutres

Minireview

Programmed cell death triggered by nucleotide pool damage and its prevention by MutT homolog-1 (MTH1) with oxidized purine nucleoside triphosphatase

Yusaku Nakabeppu*, Sugako Oka, Zijing Sheng, Daisuke Tsuchimoto, Kunihiko Sakumi

Division of Neurofunctional Genomics, Department of Immunobiology and Neuroscience, Medical Institute of Bioregulation, Kyushu University 3-1-1 Maidashi, Higashi-ku, Fukuoka 812-8582, Japan

ARTICLE INFO

Article history:
Received 3 June 2010
Accepted 4 June 2010
Available online 11 June 2010

Keywords:
8-Oxo-dGTP
2-OH-dATP
Nucleotide pool
MTH1
OGG1
MUTYH
Programmed cell death

ABSTRACT

Accumulation of oxidized bases such as 8-oxoguanine in either nuclear or mitochondrial DNA triggers various cellular dysfunctions including mutagenesis, and programmed cell death or senescence. Recent studies have revealed that oxidized nucleoside triphosphates such as 8-oxo-dGTP in the nucleotide pool are the main source of oxidized bases accumulating in the DNA of cells under oxidative stress. To counteract such deleterious effects of nucleotide pool damage, mammalian cells possess MutT homolog-1 (MTH1) with oxidized purine nucleoside triphosphatase and related enzymes, thus minimizing the accumulation of oxidized bases in cellular DNA. Depletion or increased expression of the MTH1 protein have revealed its significant roles in avoiding programmed cell death or senescence as well as mutagenesis, and accumulating evidences indicate that MTH1 is involved in suppression of degenerative disorders such as neurodegeneration.

Contents

1. Introduction

Cellular components such as lipids, proteins and nucleic acids are at high risk of being oxidized by reactive oxygen species (ROS). ROS are inevitable byproducts of electron transport in the mitochondria or other normal metabolic pathways and are also generated as useful products for various biological processes such as host defense, neurotransmission, vasodilation and signal transduction. Their production is markedly enhanced by various environmental exposures. Such oxidative damage is considered to be a major cause for various types of cellular dysfunction resulting in cell death or mutagenesis, which may in turn cause degenerative disorders and neoplasms [1].

Organisms are equipped with defense mechanisms to minimize the accumulation of ROS. For example, superoxide dismutases convert superoxide to oxygen and hydrogen peroxide and the latter is further detoxified by peroxidases or catalases. Mice lacking the *SOD2* gene encoding mitochondrial superoxide dismutase have severe abnormalities in development and growth, including cardiomyopathy and neurodegeneration [2]. Once excessive ROS

Abbreviations: 8-oxoG, 8-oxoguanine; 8-oxo-dGTP, 8-oxo-2′-deoxyguanosine triphosphate; 2-OH-A, 2-hydroxyadenine; 2-OH-dATP, 2-hydroxy-2′-deoxyadenosine triphosphate; AIF, apoptosis-inducing factor; BER, base excision repair; NO, nitric oxide; PARP, poly(ADP-ribose) polymerase; ROS, reactive oxygen species; SOD, superoxide dismutase; SSBs, single strand breaks.

* Corresponding author. Tel.: +81 92 642 6800; fax: +81 92 642 6791.
E-mail address: yusaku@bioreg.kyushu-u.ac.jp (Y. Nakabeppu).

1383-5718/$ – see front matter © 2010 Elsevier B.V. All rights reserved.
doi:10.1016/j.mrgentox.2010.06.006

accumulates in the cells, these cells can no longer avoid severe oxidative damage. Even in the presence of functional superoxide dismutases, accumulation of oxidized macromolecules in human tissues gradually occurs during normal aging; hence, oxidative damage has been implicated in aging and degenerative disorders and may well be the major cause of these disorders [1].

Among the various types of oxidative damage to cellular macromolecules, damage to nucleic acids is particularly hazardous because of the genetic information present in cellular DNAs (nuclear and mitochondrial), can be altered. Furthermore, oxidized nucleotides can disturb various cellular processes. Such oxidative damage accumulating in cells often results not only in mutagenesis, but also in programmed cell death. The former can initiate carcinogenesis in somatic cells, and mutations fixed in germ lines cause genetic polymorphisms or cause hereditary diseases with a malfunction of the gene(s), while the latter often causes degenerative diseases [3–6].

There are two pathways for the accumulation of oxidized bases in cellular DNA or RNA: one is a result of the incorporation of oxidized nucleotides generated in nucleotide pools while the other is a result of the direct oxidation of bases in DNA or RNA [7]. Recent progress in studies of the sanitization of nucleotide pools, as well as DNA repair, has revealed that the impact of oxidation of free nucleotides is unexpectedly large, in comparison with the direct oxidation of DNA [8]. In this review, we focus on the programmed cell death induced when oxidized purine nucleoside triphosphates are accumulated in the nucleotide pools and how their sanitizing enzyme MTH1 prevents such biological consequence.

2. Oxidation of purine nucleotides and their incorporation into cellular DNA

Among the nucleobases, guanine is known to be the most susceptible to oxidation and its simple oxidized form, 8-oxoguanine (8-oxoG), is one of the major oxidation products in DNA or nucleotides [9]. *In vitro* exposure of the guanine base to H_2O_2 and ascorbic acid or to $Fe(II)^{-}$-EDTA generates 8–9 times more 8-oxoG residues in the nucleotide dGTP than in DNA. Interestingly, the C-8 position of dATP is not oxidized in the treatments; instead, the C-2 position of dATP is oxidized, thus yielding 2-hydroxy-2′-deoxyadenosine triphosphate (2-OH-dATP). However, treatment with $Fe(II)^{-}$-EDTA generates 2-hydroxyadenine (2-OH-A) residues in DNA to as little as 1.5% of the level of 2-OH-A residues that are formed from dATP [10]. Free nucleotides are thus more susceptible to oxidation by ROS than is DNA.

These *in vitro* studies indicated that dGTP is likely to be most susceptible to oxidation by *in vivo* generated ROS, thus generating 8-oxo-dGTP. Although there have been few reports measuring the *in vivo* concentration of 8-oxo-dGTP in the nucleotide pool, it has recently been reported that 8-oxo-dGTP is present at 0.2–2 μM range in the mitochondrial dNTP pools of several rat tissues under normal conditions [11].

It has been established that 8-oxo-dGTP and 2-OH-dATP are frequently misinserted opposite template adenine or guanine, respectively, in DNA by various DNA polymerases for bacterial genomes, and in the nuclear and mitochondrial DNA in mammals, because of their altered base pairing properties [11–18] (Fig. 1A). 8-OxoG pairs with adenine and cytosine at equal efficiency because it prefers the *syn*-form compared with guanine, which takes mostly an *anti*-form and exclusively pairs with cytosine. However, 2-OH-A also can pair with guanine in a *syn*-form in addition to thymine. It has been shown that these oxidized nucleotides indeed increased certain mutations when they were introduced into *Escherichia coli* or mammalian cells [19,20].

As summarized in Fig. 1B, 8-oxo-dGTP is misinserted opposite template adenine as well as cytosine in DNA, thus causing mainly an A:T to C:G transversion mutation after two rounds of replication. 2-OH-dATP tends to be misinserted opposite guanine mostly, thus inducing mainly G:C to T:A transversion mutation.

3. MTH1 is a major oxidized purine nucleoside triphosphatase in mammals

E. coli mutT mutants exhibit the strongest mutator phenotype among all known *E. coli* mutator mutants and the spontaneous occurrence of A:T to C:G transversion mutation increases 1000-fold compared with wild-type. Maki and Sekiguchi demonstrated that the MutT protein hydrolyzes 8-oxo-dGTP to 8-oxo-dGMP and pyrophosphate, thus sanitizing the nucleotide pool [12]. The MutT protein also efficiently hydrolyzes 8-oxo-GTP and *mutT* mutants accumulate 8-oxoG in DNA and mRNA; 8-oxoG in the latter also results in the production of mutant proteins [21]. The *E. coli* Orf135 protein hydrolyzes 2-OH-dATP [22] and its mutants exhibit a 2-fold increase in the spontaneous occurrence of A:T to C:G transversion. The introduction of 2-OH-dATP, but not 8-oxo-dGTP or other nucleotides, into Orf135 mutants, specifically increases the mutation frequency compared with wild-type [23]. MutT and Orf135 proteins share the nudix (nucleoside diphosphate linked moiety X) motif corresponding to the 23 residues from Gly37 to Gly59 of *E. coli* MutT, which constitute the phosphohydrolase module for hydrolysis of phosphate bonds of the substrates [24,25].

We have identified a human homolog of the MutT protein and designated it as MTH1 (MutT homolog-1) [26–28]. However, it is now referred to as NUDT1 because it is the first identified protein with the nudix motif in eukaryotes. In contrast to MutT, MTH1 efficiently hydrolyzes two forms of oxidized dATP, 2-OH-dATP and 8-oxo-dATP, as well as 8-oxo-dGTP. It also hydrolyzes the corresponding ribonucleotides, 2-OH-ATP, 8-oxo-GTP and 8-oxo-ATP. Among these, MTH1 has the highest affinity to 2-OH-ATP (K_m = 4.3 μM), while the highest catalytic efficiency was observed in 2-OH-dATP (k_{cat}/K_m = 1.68 s^{-1} μM^{-1}) [29,30]. We determined the solution structure of MTH1 by multi-dimensional heteronuclear NMR spectroscopy [31]. The protein adopts a highly similar folding pattern to *E. coli* MutT, despite the low sequence similarity outside the conserved nudix motif [32]. The substrate binding pockets are dissimilar, which might account for the different substrate specificities observed for the two enzymes [33]. Based on the arrangement of the pocket-forming residues, combined with the mutagenesis data, we generated models for the substrate recognition of MTH1 in which Asn-33 and Asp-119 play pivotal roles in discriminating the oxidized form of the purine, namely 8-oxoG and 2-OH-A, while Trp-117 is important for determining the affinity with purine rings [34,35]. Among known proteins with the nudix motif, two other mammalian proteins, MTH2 (NUDT15) and NUDT5, were identified with the potential to hydrolyze either 8-oxo-dGTP or 8-oxo-(d)GDP to 8-oxo-(d)GMP, respectively [36–38]. NUDT5 also hydrolyzes 8-oxo-dADP and to a lesser extent 2-OH-dADP [39]. The discovery of NUDT5 with 8-oxo-(d)GDPase activity, further revealed that MTH1 and MutT can both hydrolyze 8-oxo-GDP [38,40]. MTH1 also recognizes oxidized forms of dATP and ATP as mentioned above. Therefore, we expect that their diphosphate forms can be hydrolyzed by MTH1, suggesting that MTH1 is the most powerful enzyme for the sanitization of nucleotide pools [8] (Fig. 1B). Gene knockdown experiments for MTH1, MTH2 and NUDT5 in cultured human cells revealed that MTH1 deficiency induced an increased occurrence of A:T to C:G transversion mutations when 8-oxo-dGTP was introduced into cells [41].

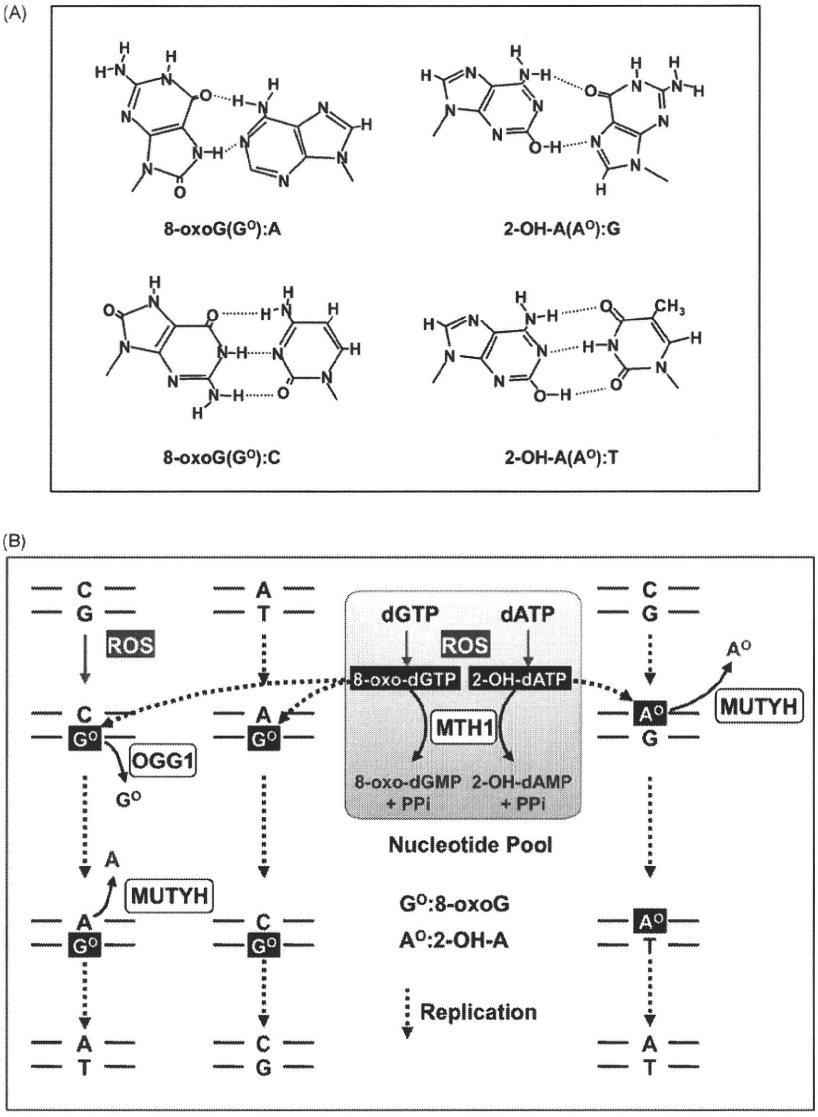

Fig. 1. Altered base pairing and mutagenesis caused by the oxidation of nucleic acids, and defense mechanisms in mammals. (A) Altered base pairing of 8-oxoguanine and 2-hydroxyadenine. During DNA replication, 8-oxoG (G^O) and 2-OH-A (A^O) can pair with adenine (A) and guanine (G) as well as with cytosine (C) or thymine (T), respectively. (B) Mutagenesis caused by 8-oxoG and 2-OH-A. 8-OxoG accumulates in DNA as a result of the incorporation of 8-oxo-dGTP from nucleotide pools or because of the direct oxidation of guanine in DNA. This buildup increases the likelihood of an A:T to C:G or G:C to T:A transversion. On the other hand, 2-OH-A is derived mainly from the incorporation of 2-OH-dATP from nucleotide pools. The accumulation of 8-oxoG or 2-OH-A in DNA is minimized through the coordinated actions of MTH1, OGG1 and MUTYH. See text for details (modified from Ref. [6] with permission).

4. MTH1 deficiency increases susceptibility to cellular dysfunction caused by ROS

We reported that lung adenomas/carcinomas developed spontaneously in 8-oxoG DNA glycosylase 1 (OGG1)-null mice at about 1.5 years after birth, and that 8-oxoG was highly accumulated in their genomes because of the lack of excision repair of 8-oxoG [42]. In that study, we found that no tumor was formed in the lungs of mice lacking both the OGG1 and MTH1 proteins, despite an increased accumulation of 8-oxoG in these mice. This observation suggests that *Mth1* gene disruption resulted in a suppression of the tumorigenesis caused by an OGG1 deficiency. If cell death is caused by the accumulation of a large amount of oxidized purine nucleoside triphosphates in nucleotide pools with MTH1 deficiency, in addition to the accumulation of 8-oxoG in cellular DNA because of the OGG1 deficiency, then cells with premutagenic lesions might not survive to produce precancerous cells with mutations in either proto-oncogenes or tumor suppressor genes. This might be why carcinogenesis is suppressed in mice lacking both the OGG1 and MTH1 proteins [43].

We have demonstrated that MTH1-null mouse embryo fibroblasts (MEF) are highly susceptible to cell dysfunction and death caused by exposure to H_2O_2, with condensed nuclei and degenerated mitochondria in which electron dense deposits were seen in place of intact cristae [44]. The cell death observed was not dependent on either poly(ADP-ribose) polymerase or caspases. A continuous accumulation of 8-oxoG, both in the nuclear and mitochondrial DNA, was observed after exposure to H_2O_2. All of the H_2O_2-induced alterations observed in MTH1-null MEFs were effectively suppressed by the expression of wild-type human MTH1 (hMTH1), while they were only partially suppressed by the expression of mutant hMTH1 which possessed either only 8-oxo-dGTPase

or 2-OH-dATPase activity. MTH1 thus protects the cells from H_2O_2-induced cell dysfunction and death by hydrolyzing oxidized purine nucleotides.

It has been shown that hMTH1 depletion in p53-proficient human cancer-derived or SV40-transformed cell lines promotes H_2O_2-induced apoptosis through a Noxa- and caspase-3/7-mediated signaling pathway [45]. In contrast, hMTH1 depletion in primary human cells results in rapid cellular senescence with an increased accumulation of 8-oxoG in genomic DNA and upregulation of tumor suppressor genes including *p53*, especially under high oxygen tension (20%) [46]. In both cases, nuclear accumulation of γ-H2AX immunoreactivity was observed, suggesting that incorporation of 8-oxoG into nuclear DNA results in double-strand breaks, thus inducing p53-dependent responses. These results indicate that the nucleotide pool is a critical target of intracellular ROS and that oxidized nucleotides, unless continuously eliminated, can rapidly induce programmed cell death or senescence [8].

5. Two distinct pathways of cell death are triggered by 8-oxoG accumulating in nuclear and mitochondrial DNAs

Under oxidative stress conditions, generation of 8-oxo-dGTP in the nucleotide pool as well as direct oxidation of guanine in DNA results in the increased accumulation of 8-oxoG in nuclear and mitochondrial DNAs [44,47], thus inducing programmed cell death or senescence (Fig. 2). However, it is not clear which form of DNA is involved—nuclear or mitochondrial—or how such programmed processes are executed. To distinguish the biological effects of 8-oxoG accumulation in nuclear or mitochondrial DNA, we established cells that accumulate 8-oxoG selectively in either type of DNA by expression of a nuclear or mitochondrial form of human OGG1 proteins. These selectively excise 8-oxoG opposite cytosines in DNA in OGG1-null mouse cells [48,49]. The increased accumulation of 8-oxoG in nuclear DNA caused poly(ADP-ribose) polymerase (PARP)-dependent nuclear translocation of apoptosis-inducing factor (AIF). On the other hand, the increased accumulation of 8-oxoG in mitochondrial DNA caused mitochondrial dysfunction followed by Ca^{2+} efflux and activation of calpains. Both types of cell death were accompanied by increased accumulation of single strand breaks (SSBs) in the respective DNAs. These were suppressed by knockdown of MUTYH that excises adenine inserted opposite 8-oxoG in DNA during replication, thus initiating base excision repair (BER). Recently, it has been shown that DNA polymerase λ efficiently insert cytosine opposite 8-oxoG after adenine excision by MUTYH, thus ensuring the faithful repair of A:8-oxoG mispairs [50]. Under increased accumulation of 8-oxoG in template DNA, however, MUTYH might induce futile BER because an adenine can be reinserted opposite an 8-oxoG during BER, thus causing accumulation of SSBs in the nascent strand [51] (Fig. 2A). Knockdown of MUTYH resulted in escape from both types of cell death, indicating that MUTYH functions as a molecular switch for the two types of programmed cell death when 8-oxoG accumulates in either nuclear or mitochondrial DNA. These results indicate that MUTYH-dependent excision of adenines paired with 8-oxoGs lead to the accumulation of SSBs in each type of DNA [48]. SSBs accumulating in nuclear DNA activate PARP followed by nuclear translocation of AIF, thus executing cell death [52,53] (Fig. 2B). In contrast, SSBs accumulating in mitochondrial DNA results in their degradation, and in mitochondrial dysfunctions such as ATP depletion and opening the membrane permeability transition pore. These lead to Ca^{2+} efflux from mitochondria causing activation of the Ca^{2+}-dependent proteases, calpains, in the cytoplasm. Activated calpains induce lysosomal rupture and cell death [54,55] (Fig. 2C).

We recently found that mice lacking MUTYH, OGG1 and MTH1 proteins are highly susceptible to the rapid development of various types of spontaneous tumors (our unpublished data), thus demonstrating that MUTYH-dependent programmed cell death is why mice lacking both OGG1 and MTH1 proteins do not develop the lung tumors observed in mice lacking only the OGG1 protein.

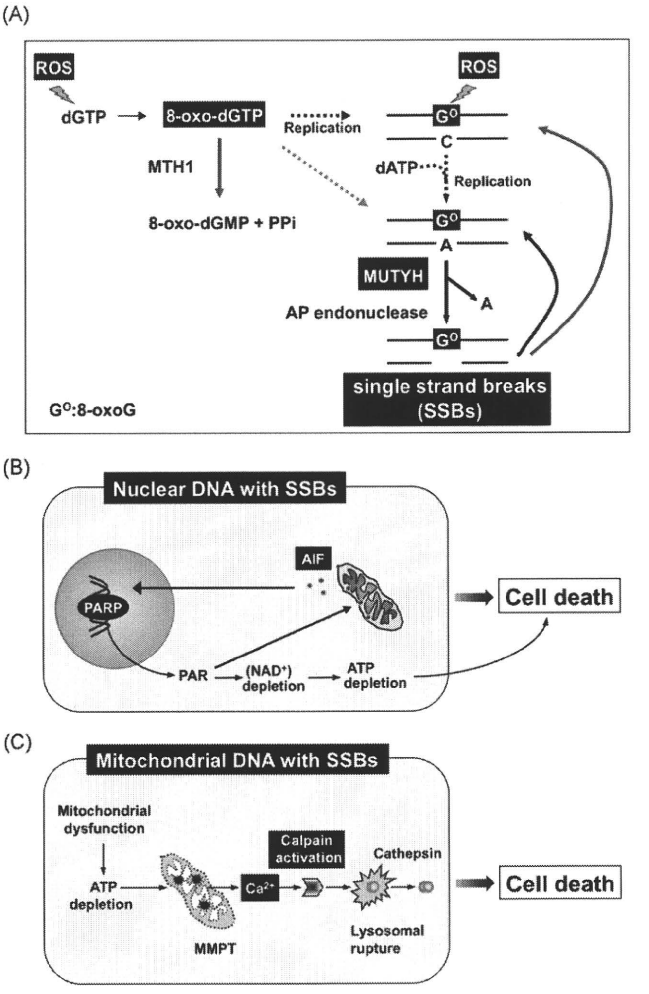

Fig. 2. MUTYH-dependent programmed cell death triggered by accumulation of 8-oxoguanine in nuclear and mitochondrial DNA. (A) Reactive oxygen species (ROS) oxidize dGTP in the nucleotide pool and, to a lesser extent, guanine in DNA. 8-Oxo-dGTP escaping from hydrolysis by MTH1 is utilized by DNA polymerases as a substrate for DNA synthesis, thus increasing the accumulation of 8-oxoG (G^O) in DNA. During the next round of replication, adenine (A) can be inserted opposite 8-oxoG in DNA, MUTYH excises the adenine in the nascent strand and AP endonucleases incise the abasic sites. Cytosine (C) or adenine may be inserted opposite 8-oxoG during repair replication; however, insertion of adenine causes futile cycle of the base excision repair (BER), thus accumulating single strand breaks (SSBs) in the nascent strand when 8-oxoG accumulates to a large extent in the template DNA. (B) When 8-oxoG accumulates highly in nuclear DNA, poly(ADP-ribose) polymerase (PARP) binds the SSBs generated by MUTYH-initiated BER, thus increasing poly(ADP-ribosyl)ation (PAR) resulting in nuclear translocation of apoptosis-inducing factor (AIF) in mitochondria. AIF executes apoptotic cell death with large chromosomal DNA fragmentation. (C) 8-OxoG accumulated highly in mitochondrial DNA causes degradation of mitochondrial DNA through MUTYH-initiated BER, thus causing mitochondrial dysfunction. Mitochondrial membrane permeability transition (MMPT) initiated by ATP depletion causes Ca^{2+} efflux from mitochondria, thus an increased Ca^{2+} in the cytoplasm activates calpains, which in turn cause lysosomal rupture to execute cell death (modified from Ref. [48] with permission).

6. Oxidation of the nucleotide pool for mitochondrial DNA causes MUTYH-dependent cell death

We reported that both 8-oxoG accumulation and the expression levels of MTH1 are highly increased in the cardiovascular tissues of a rat model of genetic hypertension compared with control rats,

suggesting that the oxidation of nucleotide pools may play a role in the development of hypertension [56]. Cardiovascular tissues are constitutively exposed to nitric oxide (NO), a vasodilator and neurotransmitter, which produces peroxynitrite in the presence of superoxide [1]. Peroxynitrite itself produces the hydroxyl radical, which is known to vigorously oxidize nucleic acids *in vitro*; however, it has not been clear whether or how NO participates in the oxidation of nucleic acids *in vivo* [57].

We examined whether hMTH1 would prevent cellular dysfunction induced by sodium nitroprusside, a spontaneous NO donor [58]. Exposure caused 8-oxoG accumulation in the DNA of proliferating MTH1-null cells, which underwent mitochondrial degeneration and subsequently died. Quiescent MTH1-null cells also died with the 8-oxoG accumulation but only when it affected mitochondrial and not nuclear DNA. In both proliferative and quiescent conditions, the accumulation of 8-oxoG in DNA and the consequent cell death were effectively prevented by hMTH1 treatment. Knockdown of MUTYH in quiescent MTH1-null cells significantly reduced cell death, suggesting that 8-oxoG incorporated into mitochondrial DNA is a main cause of this form of cell death. To verify this possibility, an artificially modified hMTH1 with a mitochondrial targeting peptide (mTP), namely mTP-EGFP-hMTH1, which localizes exclusively in mitochondria, was expressed in MTH1-null cells [58]. mTP-EGFP-hMTH1 selectively prevented the accumulation of 8-oxoG in mitochondrial, but not nuclear DNA, after exposure of proliferating cells to NO and also efficiently prevented cell death. We thus conclude that exposure of cells to NO causes oxidation of mitochondrial deoxynucleotide pools and that the buildup of oxidized bases in mitochondrial DNA initiates cell death.

It is likely that the accumulation of 8-oxoG in nuclear DNA by the incorporation of 8-oxo-dGTP from the nucleotide pools does not induce acute cell death [58]. The MUTYH protein in mammalian cells functions in a replication-coupled manner by association with proliferating cell nuclear antigen (PCNA), replication protein A (RPA) and MutS homolog 6 (MSH6) in the nucleus [59–61] and the levels of MUTYH in the nucleus increased 3- to 4-fold during progression of the cell cycle and reached maximum levels in S phase compared with levels in early G1 and that MUTYH was localized at the site of DNA replication [62]. Therefore, MUTYH in nuclei selectively recognizes and excises adenine inserted into the nascent strand opposite template 8-oxoG in DNA, but not the template adenine that pairs with 8-oxoG in nascent strand derived from 8-oxo-dGTP in the nucleotide pool. Thus, 8-oxoG derived from nucleotide pool may not result in accumulation of SSBs through MUTYH-initiated BER. It is likely that mismatch repair might recognize 8-oxoG inserted opposite template adenine in DNA [63] and OGG1 also excises 8-oxoG inserted opposite template cytosine in DNA [64,65]. However, these processes are not so efficient because 8-oxoG level in nuclear DNA in the absence of MTH1 is still high 24 h after exposure to NO, which might cause delayed cell death through further replication (Fig. 2A and B).

In mitochondria, MUTYH might function independently of replication because mitochondria lack replication coupling factors such as PCNA [43]. It has been shown that the bacterial MutY protein can excise an adenine opposite an 8-oxoG regardless of the origin of the adenine base; the template adenine that pairs with an 8-oxoG in the nascent strand derived from 8-oxo-dGTP in the nucleotide pool (Fig. 2A: gray dotted line), or adenine inserted into the nascent strand opposite template 8-oxoG [66]. Therefore, in mitochondria, MUTYH can excise adenine opposite 8-oxoG regardless of their origin, as does bacterial MutY. We thus suggest that the accumulation of 8-oxoG in mitochondrial DNA in the absence of MTH1 results in excess formation of SSBs in both strands of DNA through MUTYH-initiated BER. This would cause double-strand breaks and thereby induce mitochondrial degeneration followed by cell death (Fig. 2A and C), particularly when cells are exposed to excess NO under conditions of inflammation or excitotoxicity [58,67].

7. Neuronal accumulation of 8-oxoG causes neurodegeneration, which can be suppressed by MTH1

Oxidatively damaged bases, such as 8-oxoG accumulates in both nuclear and mitochondrial DNAs during aging [44,68,69] and such accumulation appears to increase dramatically in patients with various neurodegenerative diseases, such as Parkinson's disease (PD) [70,71], Alzheimer's disease (AD) [72,73] or amyotrophic lateral sclerosis (ALS) [74,75]. We have shown that a significant increase of 8-oxoG in mitochondrial DNA was accompanied by an elevated expression of MTH1 [71], the mitochondrial form of OGG1 (OGG1-2a) [76] and an N-terminally truncated form of MUTYH encoded by an alternatively spliced *MUTYH* mRNA in the substantia nigra neurons of patients with PD [77]. In postmortem tissue specimens from patients with AD, the expression levels of MTH1 in the entorhinal cortex were also elevated, whilst the levels of MTH1 apparently decreased in the stratum lucidum at CA3, corresponding to mossy fiber synapses, where MTH1 was highly expressed in the control subjects [78]. In contrast, expression level of OGG1-2a was found to decrease in the orbitofrontal gyrus and the entorhinal cortex in patients with AD compared with control subjects [79]. The accumulation of 8-oxoG was increased in most of the large motor neurons in patients with ALS, with a decreased expression of OGG1-2a but not MTH1. It is thus likely that OGG1-2a is indeed unstable under increased oxidative stress, compared with MTH1 [75].

We reported that the levels of 8-oxoG in cellular DNA and RNA increased in the mouse nigrostriatal system during tyrosine hydroxylase (TH)-positive dopamine neuron loss induced by the administration of 1-methyl-4-phenyl-1,2,3,6-tetrahydropyridine (MPTP) [80]. In contrast to wild-type mice, MTH1-null mice exhibited a greater accumulation of 8-oxoG in mitochondrial DNA, accompanied by a more significant decrease in TH- and dopamine transporter-positive fibers in the striatum after MPTP administration [80]. We thus demonstrated that MTH1 indeed protects the dopaminergic neurons from oxidative damage in nucleotide pools. This was especially effected by preventing 8-oxoG accumulation in the mitochondrial DNA of striatal nerve terminals of dopaminergic neurons [81], which is likely to cause mitochondrial dysfunction through the MUTYH-initiated BER as shown in Fig. 2A and C.

Recently, a transgenic mouse has been established in which the human MTH1 is expressed [82]. Wild-type mice exposed to 3-nitropropionic acid, an inhibitor for mitochondrial succinate dehydrogenase, develop neuropathological and behavioral symptoms that resemble those of Huntington's disease, with an increased 8-oxoG accumulation in medium spiny neurons in striatum. hMTH1 transgene expression conferred a dramatic protection against these Huntington's disease-like symptoms, including weight loss, dystonia and gait abnormalities, striatal degeneration and death [82]. The findings indicate that oxidized nucleoside triphosphates such as 8-oxo-dGTP accumulating in nucleotide pools in medium spiny neurons have a significant contribution to their degeneration.

Enhanced oxidative stress has been implicated in the excitotoxicity of the central nervous system and 8-oxoG was reported to be accumulated in the rat hippocampus after administration of kainate, an excitotoxin for glutamate receptors [83]. We reported that the 8-oxoG levels in mitochondrial DNA and cellular RNA increased significantly in the CA3 subregion of the mouse hippocampus 6–12 h after kainate administration but returned to basal levels within a few days [67]. 8-OxoG accumulation in mitochondrial DNA was remarkable in CA3 microglia, whereas that in nuclear DNA or cellular RNA was also detected in the CA3 pyrami-

dal cells and astrocytes. MTH1-null and wild-type mice exhibited a similar degree of CA3 neuron loss after kainate administration; however, the 8-oxoG levels that accumulated in mitochondrial DNA and cellular RNA in the CA3 microglia increased significantly in the MTH1-null mice in comparison with wild-type mice [67]. This demonstrated that MTH1 efficiently suppresses the accumulation of 8-oxoG in both cellular DNA and RNA in the hippocampus—especially in microglia—caused by the excitotoxicity that plays a major role during neurodegeneration [84].

We examined the expression levels of MTH1 and OGG1 in the mouse hippocampus after kainate administration. The *Mth1* mRNA level decreased soon after kainate administration and then quickly recovered beyond the basal level. A continuously raised MTH1 protein level was observed, whereas the *Ogg1* mRNA level remained constant [67]. These results may indicate that oxidative stress in brain induces expression of MTH1 especially in microglia, thus avoiding cellular dysfunction.

8. Future perspectives

Oxidative DNA damage has been considered as one of major threats for organisms, causing mutagenesis and carcinogenesis [5]. Because bases of free nucleotides in the nucleotide pools are more susceptible to oxidation by ROS, compared with those in DNA, oxidized nucleotides generated in the nucleotide pools have greater impact as causes for mutagenesis through their incorporation into DNA. Beyond mutagenesis, the incorporation of oxidized nucleotides into nuclear or mitochondrial DNA from the damaged nucleotide pools triggers programmed processes resulting in cell death or senescence. Such programmed processes are involved in tumor suppression or neurodegeneration in animal models [67,80,82]. MTH1, a major sanitizing enzyme for oxidized nucleotide pools plays a crucial role by suppressing their accumulation in cellular DNA. In addition to oxidized purine deoxyribonucleoside triphosphates, MTH1 efficiently hydrolyzes oxidized purine ribonucleoside triphosphates such as 2-OH-ATP, 8-oxo-ATP and, to a lesser extent, 8-oxo-GTP. As a result, cellular dysfunction may also be caused by their incorporation into RNA. Alternatively, such oxidized purine ribonucleoside triphosphates might interfere with various pathways of signal transduction or metabolisms in which ATP or GTP function as essential mediators of co-factors, thus suggesting that free forms of oxidized purine nucleotides might themselves exert a certain degree of cytotoxicity.

Conflict of interest statement

There is no conflicting interest.

Acknowledgments

This work was supported by grants from the Ministry of Education, Culture, Sports, Science and Technology of Japan [20013034 to Y.N., 20012038 to K.S.]; the Japan Society for the Promotion of Science [19390114 to D.T.] and Kyushu University Global COE program [Y.N., Z.S.].

References

[1] M. Valko, D. Leibfritz, J. Moncol, M.T. Cronin, M. Mazur, J. Telser, Free radicals and antioxidants in normal physiological functions and human disease, Int. J. Biochem. Cell Biol. 39 (2007) 44–84.
[2] R.M. Lebovitz, H. Zhang, H. Vogel, J. Cartwright Jr., L. Dionne, N. Lu, S. Huang, M.M. Matzuk, Neurodegeneration, myocardial injury, and perinatal death in mitochondrial superoxide dismutase-deficient mice, Proc. Natl. Acad. Sci. U.S.A. 93 (1996) 9782–9787.
[3] A Sakai, M. Nakanishi, K. Yoshiyama, H. Maki, Impact of reactive oxygen species on spontaneous mutagenesis in *Escherichia coli*, Genes Cells 11 (2006) 767–778.
[4] M. Ohno, T. Miura, M. Furuichi, Y. Tominaga, D. Tsuchimoto, K. Sakumi, Y. Nakabeppu, A genome-wide distribution of 8-oxoguanine correlates with the preferred regions for recombination and single nucleotide polymorphism in the human genome, Genome Res. 16 (2006) 567–575.
[5] Y. Nakabeppu, K. Sakumi, K. Sakamoto, D. Tsuchimoto, T. Tsuzuki, Y. Nakatsu, Mutagenesis and carcinogenesis caused by the oxidation of nucleic acids, Biol. Chem. 387 (2006) 373–379.
[6] Y. Nakabeppu, D. Tsuchimoto, H. Yamaguchi, K. Sakumi, Oxidative damage in nucleic acids and Parkinson's disease, J. Neurosci. Res. 85 (2007) 919–934.
[7] Y. Nakabeppu, D. Tsuchimoto, M. Furuichi, K. Sakumi, The defense mechanisms in mammalian cells against oxidative damage in nucleic acids and their involvement in the suppression of mutagenesis and cell death, Free Radic. Res. 38 (2004) 423–429.
[8] Y. Nakabeppu, M. Behmanesh, H. Yamaguchi, D. Yoshimura, K. Sakumi, Prevention of the mutagenecity and cytotoxicity of oxidized purine nucleotides, in: M.D. Evans, M.S. Cooke (Eds.), Oxidative Damage to Nucleic Acids, Landes Bioscience/Springer, Austin, TX/New York, NY, USA, 2007, pp. 40–53.
[9] H. Kasai, S. Nishimura, Hydroxylation of deoxyguanosine at the C-8 position by ascorbic acid and other reducing agents, Nucleic Acids Res. 12 (1984) 2137–2145.
[10] H. Kamiya, H. Kasai, Formation of 2-hydroxydeoxyadenosine triphosphate, an oxidatively damaged nucleotide, and its incorporation by DNA polymerases. Steady-state kinetics of the incorporation, J. Biol. Chem. 270 (1995) 19446–19450.
[11] Z.F. Pursell, J.T. McDonald, C.K. Mathews, T.A. Kunkel, Trace amounts of 8-oxo-dGTP in mitochondrial dNTP pools reduce DNA polymerase gamma replication fidelity, Nucleic Acids Res. 36 (2008) 2174–2181.
[12] H. Maki, M. Sekiguchi, MutT protein specifically hydrolyses a potent mutagenic substrate for DNA synthesis, Nature 355 (1992) 273–275.
[13] K. Satou, H. Harashima, H. Kamiya, Mutagenic effects of 2-hydroxy-dATP on replication in a HeLa extract: induction of substitution and deletion mutations, Nucleic Acids Res. 31 (2003) 2570–2575.
[14] M. Yamada, T. Nunoshiba, M. Shimizu, P. Gruz, H. Kamiya, H. Harashima, T. Nohmi, Involvement of Y-family DNA polymerases in mutagenesis caused by oxidized nucleotides in *Escherichia coli*, J. Bacteriol. 188 (2006) 4992–4995.
[15] M. Shimizu, P. Gruz, H. Kamiya, C. Masutani, Y. Xu, Y. Usui, H. Sugiyama, H. Harashima, F. Hanaoka, T. Nohmi, Efficient and erroneous incorporation of oxidized DNA precursors by human DNA polymerase η, Biochemistry 46 (2007) 5515–5522.
[16] M.A. Graziewicz, R.J. Bienstock, W.C. Copeland, The DNA polymerase γ Y955C disease variant associated with PEO and parkinsonism mediates the incorporation and translesion synthesis opposite 7,8-dihydro-8-oxo-2′-deoxyguanosine, Hum. Mol. Genet. 16 (2007) 2729–2739.
[17] J.N. Patro, M. Urban, R.D. Kuchta, Interaction of human DNA polymerase α and DNA polymerase I from *Bacillus stearothermophilus* with hypoxanthine and 8-oxoguanine nucleotides, Biochemistry 48 (2009) 8271–8278.
[18] A. Katafuchi, A. Sassa, N. Niimi, P. Grúz, H. Fujimoto, C. Masutani, F. Hanaoka, T. Ohta, T. Nohmi, Critical amino acids in human DNA polymerases η and κ involved in erroneous incorporation of oxidized nucleotides, Nucleic Acids Res. 38 (2010) 859–867.
[19] K. Satou, M. Yamada, T. Nohmi, H. Harashima, H. Kamiya, Mutagenesis induced by oxidized DNA precursors: roles of Y family DNA polymerases in *Escherichia coli*, Chem. Res. Toxicol. 18 (2005) 1271–1278.
[20] K. Satou, K. Kawai, H. Kasai, H. Harashima, H. Kamiya, Mutagenic effects of 8-hydroxy-dGTP in live mammalian cells, Free Radic. Biol. Med. 42 (2007) 1552–1560.
[21] F. Taddei, H. Hayakawa, M. Bouton, A. Cirinesi, I. Matic, M. Sekiguchi, M. Radman, Counteraction by MutT protein of transcriptional errors caused by oxidative damage, Science 278 (1997) 128–130.
[22] H. Kamiya, N. Murata-Kamiya, E. Iida, H. Harashima, Hydrolysis of oxidized nucleotides by the *Escherichia coli* Orf135 protein, Biochem. Biophys. Res. Commun. 288 (2001) 499–502.
[23] H. Kamiya, E. Iida, N. Murata-Kamiya, Y. Yamamoto, T. Miki, H. Harashima, Suppression of spontaneous and hydrogen peroxide-induced mutations by a MutT-type nucleotide pool sanitization enzyme, the *Escherichia coli* Orf135 protein, Genes Cells 8 (2003) 941–950.
[24] H. Shimokawa, Y. Fujii, M. Furuichi, M. Sekiguchi, Y. Nakabeppu, Functional significance of conserved residues in the phosphohydrolase module of *Escherichia coli* MutT protein, Nucleic Acids Res. 28 (2000) 3240–3249.
[25] S.F. O'Handley, C.A. Dunn, M.J. Bessman, Orf135 from *Escherichia coli* is a Nudix hydrolase specific for CTP, dCTP, and 5-methyl-dCTP, J. Biol. Chem. 276 (2001) 5421–5426.
[26] K. Sakumi, M. Furuichi, T. Tsuzuki, T. Kakuma, S. Kawabata, H. Maki, M. Sekiguchi, Cloning and expression of cDNA for a human enzyme that hydrolyzes 8-oxo-dGTP, a mutagenic substrate for DNA synthesis, J. Biol. Chem. 268 (1993) 23524–23530.
[27] M. Furuichi, M.C. Yoshida, H. Oda, T. Tajiri, Y. Nakabeppu, T. Tsuzuki, M. Sekiguchi, Genomic structure and chromosome location of the human *mutT* homologue gene *MTH1* encoding 8-oxo-dGTPase for prevention of A:T to C:G transversion, Genomics 24 (1994) 485–490.
[28] Y. Nakabeppu, Molecular genetics and structural biology of human MutT homolog, MTH1, Mutat. Res. 477 (2001) 59–70.
[29] K. Fujikawa, H. Kamiya, H. Yakushiji, Y. Fujii, Y. Nakabeppu, H. Kasai, The oxidized forms of dATP are substrates for the human MutT homologue, the hMTH1 protein, J. Biol. Chem. 274 (1999) 18201–18205.

[30] K. Fujikawa, H. Kamiya, H. Yakushiji, Y. Nakabeppu, H. Kasai, Human MTH1 protein hydrolyzes the oxidized ribonucleotide, 2-hydroxy-ATP, Nucleic Acids Res. 29 (2001) 449–454.
[31] M. Mishima, Y. Sakai, N. Itoh, H. Kamiya, M. Furuichi, M. Takahashi, Y. Yamagata, S. Iwai, Y. Nakabeppu, M. Shirakawa, Structure of human MTH1, a Nudix family hydrolase that selectively degrades oxidized purine nucleoside triphosphates, J. Biol. Chem. 279 (2004) 33806–33815.
[32] H. Yakushiji, F. Maraboeuf, M. Takahashi, Z.S. Deng, S. Kawabata, Y. Nakabeppu, M. Sekiguchi, Biochemical and physicochemical characterization of normal and variant forms of human MTH1 protein with antimutagenic activity, Mutat. Res. 384 (1997) 181–194.
[33] T. Nakamura, S. Meshitsuka, S. Kitagawa, N. Abe, J. Yamada, T. Ishino, H. Nakano, T. Tsuzuki, T. Doi, Y. Kobayashi, S. Fujii, M. Sekiguchi, Y. Yamagata, Structural and dynamic features of the MutT protein in the recognition of nucleotides with the mutagenic 8-oxoguanine base, J. Biol. Chem. 285 (2010) 444–452.
[34] Y. Sakai, M. Furuichi, M. Takahashi, M. Mishima, S. Iwai, M. Shirakawa, Y. Nakabeppu, A molecular basis for the selective recognition of 2-hydroxy-dATP and 8-oxo-dGTP by human MTH1, J. Biol. Chem. 277 (2002) 8579–8587.
[35] M. Takahashi, F. Maraboeuf, Y. Sakai, H. Yakushiji, M. Mishima, M. Shirakawa, S. Iwai, H. Hayakawa, M. Sekiguchi, Y. Nakabeppu, Role of tryptophan residues in the recognition of mutagenic oxidized nucleotides by human antimutator MTH1 protein, J. Mol. Biol. 319 (2002) 129–139.
[36] J.P. Cai, T. Ishibashi, Y. Takagi, H. Hayakawa, M. Sekiguchi, Mouse MTH2 protein which prevents mutations caused by 8-oxoguanine nucleotides, Biochem. Biophys. Res. Commun. 305 (2003) 1073–1077.
[37] T. Ishibashi, H. Hayakawa, M. Sekiguchi, A novel mechanism for preventing mutations caused by oxidation of guanine nucleotides, EMBO Rep. 4 (2003) 479–483.
[38] T. Ishibashi, H. Hayakawa, R. Ito, M. Miyazawa, Y. Yamagata, M. Sekiguchi, Mammalian enzymes for preventing transcriptional errors caused by oxidative damage, Nucleic Acids Res. 33 (2005) 3779–3784.
[39] H. Kamiya, M. Hori, T. Arimori, M. Sekiguchi, Y. Yamagata, H. Harashima, NUDT5 hydrolyzes oxidized deoxyribonucleoside diphosphates with broad substrate specificity, DNA Repair 8 (2009) 1250–1254.
[40] R. Ito, H. Hayakawa, M. Sekiguchi, T. Ishibashi, Multiple enzyme activities of *Escherichia coli* MutT protein for sanitization of DNA and RNA precursor pools, Biochemistry 44 (2005) 6670–6674.
[41] M. Hori, K. Satou, H. Harashima, H. Kamiya, Suppression of mutagenesis by 8-hydroxy-2′-deoxyguanosine 5′-triphosphate (7,8-dihydro-8-oxo-2′-deoxyguanosine 5′-triphosphate) by human MTH1, MTH2, and NUDT5, Free Radic. Biol. Med. 48 (2010) 1197–1201.
[42] K. Sakumi, Y. Tominaga, M. Furuichi, P. Xu, T. Tsuzuki, M. Sekiguchi, Y. Nakabeppu, Ogg1 knockout-associated lung tumorigenesis and its suppression by Mth1 gene disruption, Cancer Res. 63 (2003) 902–905.
[43] Y. Nakabeppu, D. Tsuchimoto, A. Ichinoe, M. Ohno, Y. Ide, S. Hirano, D. Yoshimura, Y. Tominaga, M. Furuichi, K. Sakumi, Biological significance of the defense mechanisms against oxidative damage in nucleic acids caused by reactive oxygen species: from mitochondria to nuclei, Ann. N.Y. Acad. Sci. 1011 (2004) 101–111.
[44] D. Yoshimura, K. Sakumi, M. Ohno, Y. Sakai, M. Furuichi, S. Iwai, Y. Nakabeppu, An oxidized purine nucleoside triphosphatase, MTH1, suppresses cell death caused by oxidative stress, J. Biol. Chem. 278 (2003) 37965–37973.
[45] C.K. Youn, J.Y. Jun, J.W. Hyun, G. Hwang, B.R. Lee, M.H. Chung, I.Y. Chang, H.J. You, hMTH1 depletion promotes oxidative-stress-induced apoptosis through a Noxa- and caspase-3/7-mediated signaling pathway, DNA Repair 7 (2008) 1809–1823.
[46] P. Rai, T.T. Onder, J.J. Young, J.L. McFaline, B. Pang, P.C. Dedon, R.A. Weinberg, Continuous elimination of oxidized nucleotides is necessary to prevent rapid onset of cellular senescence, Proc. Natl. Acad. Sci. U.S.A. 106 (2009) 169–174.
[47] M. Ohno, S. Oka, Y. Nakabeppu, Quantitative analysis of oxidized Guanine, 8-oxoguanine, in mitochondrial DNA by immunofluorescence method, Methods Mol. Biol. 554 (2009) 199–212.
[48] S. Oka, M. Ohno, D. Tsuchimoto, K. Sakumi, M. Furuichi, Y. Nakabeppu, Two distinct pathways of cell death triggered by oxidative damage to nuclear and mitochondrial DNAs, EMBO J. 27 (2008) 421–432.
[49] S. Oka, M. Ohno, Y. Nakabeppu, Construction and characterization of a cell line deficient in repair of mitochondrial, but not nuclear, oxidative DNA damage, Methods Mol. Biol. 554 (2009) 251–264.
[50] B. van Loon, U. Hubscher, An 8-oxo-guanine repair pathway coordinated by MUTYH glycosylase and DNA polymerase lambda, Proc. Natl. Acad. Sci. U.S.A. 106 (2009) 18201–18206.
[51] K. Hashimoto, Y. Tominaga, Y. Nakabeppu, M. Moriya, Futile short-patch DNA base excision repair of adenine:8-oxoguanine mispair, Nucleic Acids Res. 32 (2004) 5928–5934.
[52] S.W. Yu, S.A. Andrabi, H. Wang, N.S. Kim, G.G. Poirier, T.M. Dawson, V.L. Dawson, Apoptosis-inducing factor mediates poly(ADP-ribose) (PAR) polymer-induced cell death, Proc. Natl. Acad. Sci. U.S.A. 103 (2006) 18314–18319.
[53] J.T. Heeres, P.J. Hergenrother, Poly(ADP-ribose) makes a date with death, Curr. Opin. Chem. Biol. 11 (2007) 644–653.
[54] K.K. Wang, Calpain and caspase: can you tell the difference? Trends Neurosci. 23 (2000) 20–26.
[55] T. Yamashima, S. Oikawa, The role of lysosomal rupture in neuronal death, Prog. Neurobiol. 89 (2009) 343–358.
[56] T. Ohtsubo, Y. Ohya, Y. Nakamura, Y. Kansui, M. Furuichi, K. Matsumura, K. Fujii, M. Iida, Y. Nakabeppu, Accumulation of 8-oxo-deoxyguanosine in cardiovascular tissues with the development of hypertension, DNA Repair 6 (2007) 760–769.
[57] J.C. Niles, J.S. Wishnok, S.R. Tannenbaum, Peroxynitrite-induced oxidation and nitration products of guanine and 8-oxoguanine: structures and mechanisms of product formation, Nitric Oxide 14 (2006) 109–121.
[58] J. Ichikawa, D. Tsuchimoto, S. Oka, M. Ohno, M. Furuichi, K. Sakumi, Y. Nakabeppu, Oxidation of mitochondrial deoxynucleotide pools by exposure to sodium nitroprusside induces cell death, DNA Repair 7 (2008) 418–430.
[59] A. Parker, Y. Gu, W. Mahoney, S.H. Lee, K.K. Singh, A.L. Lu, Human homolog of the MutY repair protein (hMYH) physically interacts with proteins involved in long patch DNA base excision repair, J. Biol. Chem. 276 (2001) 5547–5555.
[60] Y. Gu, A. Parker, T.M. Wilson, H. Bai, D.Y. Chang, A.L. Lu, Human MutY homolog, a DNA glycosylase involved in base excision repair, physically and functionally interacts with mismatch repair proteins human MutS homolog 2/human MutS homolog 6, J. Biol. Chem. 277 (2002) 11135–11142.
[61] H. Hayashi, Y. Tominaga, S. Hirano, A.E. McKenna, Y. Nakabeppu, Y. Matsumoto, Replication-associated repair of adenine:8-oxoguanine mispairs by MYH, Curr. Biol. 12 (2002) 335–339.
[62] I. Boldogh, D. Milligan, M.S. Lee, H. Bassett, R.S. Lloyd, A.K. McCullough, hMYH cell cycle-dependent expression, subcellular localization and association with replication foci: evidence suggesting replication-coupled repair of adenine:8-oxoguanine mispairs, Nucleic Acids Res. 29 (2001) 2802–2809.
[63] M.T. Russo, M.F. Blasi, F. Chiera, P. Fortini, P. Degan, P. Macpherson, M. Furuichi, Y. Nakabeppu, P. Karran, G. Aquilina, M. Bignami, The oxidized deoxynucleoside triphosphate pool is a significant contributor to genetic instability in mismatch repair-deficient cells, Mol. Cell. Biol. 24 (2004) 465–474.
[64] K. Nishioka, T. Ohtsubo, H. Oda, T. Fujiwara, D. Kang, K. Sugimachi, Y. Nakabeppu, Expression and differential intracellular localization of two major forms of human 8-oxoguanine DNA glycosylase encoded by alternatively spliced OGG1 mRNAs, Mol. Biol. Cell 10 (1999) 1637–1652.
[65] A. Klungland, I. Rosewell, S. Hollenbach, E. Larsen, G. Daly, B. Epe, E. Seeberg, T. Lindahl, D.E. Barnes, Accumulation of premutagenic DNA lesions in mice defective in removal of oxidative base damage, Proc. Natl. Acad. Sci. U.S.A. 96 (1999) 13300–13305.
[66] T. Tajiri, H. Maki, M. Sekiguchi, Functional cooperation of MutT, MutM and MutY proteins in preventing mutations caused by spontaneous oxidation of guanine nucleotide in *Escherichia coli*, Mutat. Res. 336 (1995) 257–267.
[67] K. Kajitani, H. Yamaguchi, Y. Dan, M. Furuichi, D. Kang, Y. Nakabeppu, MTH1, an oxidized purine nucleoside triphosphatase, suppresses the accumulation of oxidative damage of nucleic acids in the hippocampal microglia during kainate-induced excitotoxicity, J. Neurosci. 26 (2006) 1688–1698.
[68] B.N Ames, M.K. Shigenaga, T.M. Hagen, Oxidants, antioxidants, and the degenerative diseases of aging, Proc. Natl. Acad. Sci. U.S.A. 90 (1993) 7915–7922.
[69] K.B. Beckman, B.N. Ames, Oxidative decay of DNA, J. Biol. Chem. 272 (1997) 19633–19636.
[70] Z.I. Alam, A. Jenner, S.E. Daniel, A.J. Lees, N. Cairns, C.D. Marsden, P. Jenner, B. Halliwell, Oxidative DNA damage in the parkinsonian brain: an apparent selective increase in 8-hydroxyguanine levels in substantia nigra, J. Neurochem. 69 (1997) 1196–1203.
[71] H. Shimura-Miura, N. Hattori, D. Kang, K. Miyako, Y. Nakabeppu, Y. Mizuno, Increased 8-oxo-dGTPase in the mitochondria of substantia nigral neurons in Parkinson's disease, Ann Neurol 46 (1999) 920–924.
[72] P. Mecocci, M.F. Beal, R. Cecchetti, M.C. Polidori, A. Cherubini, F. Chionne, L. Avellini, G. Romano, U. Senin, Mitochondrial membrane fluidity and oxidative damage to mitochondrial DNA in aged and AD human brain, Mol. Chem. Neuropathol. 31 (1997) 53–64.
[73] M.A. Lovell, W.R. Markesbery, Ratio of 8-hydroxyguanine in intact DNA to free 8-hydroxyguanine is increased in Alzheimer disease ventricular cerebrospinal fluid, Arch. Neurol. 58 (2001) 392–396.
[74] R.J. Ferrante, S.E. Browne, L.A. Shinobu, A.C. Bowling, M.J. Baik, U. MacGarvey, N.W. Kowall, R.H. Brown Jr., M.F. Beal, Evidence of increased oxidative damage in both sporadic and familial amyotrophic lateral sclerosis, J. Neurochem. 69 (1997) 2064–2074.
[75] H. Kikuchi, A. Furuta, K. Nishioka, S.O. Suzuki, Y. Nakabeppu, T. Iwaki, Impairment of mitochondrial DNA repair enzymes against accumulation of 8-oxo-guanine in the spinal motor neurons of amyotrophic lateral sclerosis, Acta Neuropathol. (Berl.) 103 (2002) 408–414.
[76] J. Fukae, M. Takanashi, S. Kubo, K. Nishioka, Y. Nakabeppu, H. Mori, Y. Mizuno, N. Hattori, Expression of 8-oxoguanine DNA glycosylase (OGG1) in Parkinson's disease and related neurodegenerative disorders, Acta Neuropathol. 109 (2005) 256–262.
[77] T. Arai, J. Fukae, T. Hatano, S. Kubo, T. Ohtsubo, Y. Nakabeppu, H. Mori, Y. Mizuno, N. Hattori, Up-regulation of hMUTYH, a DNA repair enzyme, in the mitochondria of substantia nigra in Parkinson's disease, Acta Neuropathol. 112 (2006) 139–145.
[78] A Furuta, T. Iida, Y. Nakabeppu, T. Iwaki, Expression of hMTH1 in the hippocampi of control and Alzheimer's disease, Neuroreport 12 (2001) 2895–2899.
[79] T. Iida, A. Furuta, K. Nishioka, Y. Nakabeppu, T. Iwaki, Expression of 8-oxoguanine DNA glycosylase is reduced and associated with neurofibrillary tangles in Alzheimer's disease brain, Acta Neuropathol. 103 (2002) 20–25.
[80] H. Yamaguchi, K. Kajitani, Y. Dan, M. Furuichi, M. Ohno, K. Sakumi, D. Kang, Y. Nakabeppu, MTH1, an oxidized purine nucleoside triphosphatase, protects the dopamine neurons from oxidative damage in nucleic acids caused by 1-methyl-4-phenyl-1,2,3,6-tetrahydropyridine, Cell Death Differ. 13 (2006) 551–563.

[81] Y. Nakabeppu, K. Kajitani, K. Sakamoto, H. Yamaguchi, D. Tsuchimoto, MTH1, an oxidized purine nucleoside triphosphatase, prevents the cytotoxicity and neurotoxicity of oxidized purine nucleotides, DNA Repair 5 (2006) 761–772.
[82] G. De Luca, M.T. Russo, P. Degan, C. Tiveron, A. Zijno, E. Meccia, I. Ventura, E. Mattei, Y. Nakabeppu, M. Crescenzi, R. Pepponi, A. Pezzola, P. Popoli, M. Bignami, A role for oxidized DNA precursors in Huntington's disease-like striatal neurodegeneration, PLoS Genet. 4 (2008) e1000266.
[83] M. Penkowa, S. Florit, M. Giralt, A. Quintana, A. Molinero, J. Carrasco, J. Hidalgo, Metallothionein reduces central nervous system inflammation, neurodegeneration, and cell death following kainic acid-induced epileptic seizures, J. Neurosci. Res. 79 (2005) 522–534.
[84] E.K Michaelis, Molecular biology of glutamate receptors in the central nervous system and their role in excitotoxicity, oxidative stress and aging, Prog. Neurobiol. 54 (1998) 369–415.

Nucleic Acids Research Advance Access published April 12, 2010

Nucleic Acids Research, 2010, 1–10
doi:10.1093/nar/gkq249

NUDT16 is a (deoxy)inosine diphosphatase, and its deficiency induces accumulation of single-strand breaks in nuclear DNA and growth arrest

Teruaki Iyama, Nona Abolhassani, Daisuke Tsuchimoto*, Mari Nonaka and Yusaku Nakabeppu

Division of Neurofunctional Genomics, Department of Immunobiology and Neuroscience, Medical Institute of Bioregulation, Kyushu University, 3-1-1 Maidashi, Higashi-ku, Fukuoka, 812-8582, Japan

Received December 29, 2009; Revised February 26, 2010; Accepted March 24, 2010

ABSTRACT

Nucleotides function in a variety of biological reactions; however, they can undergo various chemical modifications. Such modified nucleotides may be toxic to cells if not eliminated from the nucleotide pools. We performed a screen for modified-nucleotide binding proteins and identified human nucleoside diphosphate linked moiety X-type motif 16 (NUDT16) protein as an inosine triphosphate (ITP)/xanthosine triphosphate (XTP)/GTP-binding protein. Recombinant NUDT16 hydrolyzes purine nucleoside diphosphates to the corresponding nucleoside monophosphates. Among 29 nucleotides examined, the highest k_{cat}/K_m values were for inosine diphosphate (IDP) and deoxyinosine diphosphate (dIDP). Moreover, NUDT16 moderately hydrolyzes (deoxy)inosine triphosphate ([d]ITP). NUDT16 is mostly localized in the nucleus, and especially in the nucleolus. Knockdown of *NUDT16* in HeLa MR cells caused cell cycle arrest in S-phase, reduced cell proliferation, increased accumulation of single-strand breaks in nuclear DNA as well as increased levels of inosine in RNA. We thus concluded that NUDT16 is a (deoxy)inosine diphosphatase that may function mainly in the nucleus to protect cells from deleterious effects of (d)ITP.

INTRODUCTION

Intracellular free nucleotides play essential roles as precursors in the synthesis of DNA and RNA, and as molecules for energy storage, cofactors of metabolic pathways and regulators of signal transduction. Free nucleotides can, however, undergo various chemical modifications by endogenous and exogenous reactive molecules, some of which are inevitably produced in living cells. Chemical modifications may alter the properties of nucleotides, including their interaction with other molecules (1). Some modified deoxynucleotides are known to be incorporated into and to accumulate in newly synthesized DNA during DNA replication. Modified nucleotides, accumulated in either the nucleotide pool or DNA, may inhibit DNA or RNA polymerases during replication or transcription, reduce polymerase fidelity or alter the DNA structure, thus resulting in mutagenesis and carcinogenesis (2,3), cell death and degenerative disorders (4,5) or senescence and aging (6). In addition to DNA metabolism, the other biological functions of canonical nucleotides may also be adversely affected by modified nucleotides. Therefore, because modified nucleotides are constantly generated under physiological conditions, it is crucially important to understand how they are eliminated from cells.

It had been established that cells are equipped with specific enzymes to hydrolyze modified nucleoside triphosphates to the corresponding monophosphates to avoid their deleterious effects (4,7). Deoxyuridine triphosphatase (dUTPase), for example, hydrolyzes dUTP, thus preventing its incorporation into DNA. We have previously demonstrated that MTH1 hydrolyzes oxidized purine nucleoside triphosphates, such as 8-oxo-2′-deoxyguanosine triphosphate (8-oxo-dGTP) or 8-oxoGTP and prevents their incorporation into DNA or RNA (4).

Deamination of purine bases is one of the major chemical modifications that occurs to nucleotides under physiological conditions (8). Deamination of adenine at C6 or guanine at C2 generates hypoxanthine or xanthine, respectively, suggesting that (deoxy)inosine triphosphate ([d]ITP) and (deoxy)xanthosine triphosphate ([d]XTP) can be generated from (d)ATP and (d)GTP,

*To whom correspondence should be addressed. Tel: +81 92 642 6802; Fax: +81 92 642 6804; Email: daisuke@bioreg.kyushu-u.ac.jp

respectively. Moreover, IMP is abundant in cells as a normal intermediate of *de novo* synthesis of purine nucleotides (9), and most cells can generate IDP or ITP from IMP (10). If IDP is converted to dIDP by ribonucleotide reductase, increased dITP levels will result (11). Incorporation of such deaminated purine nucleotides into DNA or RNA causes genomic mutations or synthesis of abnormal proteins because hypoxanthine and xanthine can mis-pair with cytosine or thymine (12,13).

In human and rodents, ITPA, an inosine triphosphatase (ITPase), has been reported to hydrolyze (d)ITP and XTP to the corresponding nucleoside monophosphates and pyrophosphates (14,15). We have previously reported that *Itpa* knockout (KO) mice die before weaning with features of growth retardation and heart failure. In addition, these mice show accumulation of IMP in cellular RNA in various tissues or accumulation of ITP in the nucleotide pool of erythrocytes (16). The heart failure in *Itpa*-KO mice suggests that an accumulation of ITP in the nucleotide pool might impair some functions of adenosine triphosphate (ATP), such as ATP-dependent actomyosin contraction (17). In humans, some variants of *ITPA* are reported to be associated with decreased ITPase activity (18,19). In erythrocytes of ITPA-deficient individuals, it was established that the level of ITP, which is not detected in normal individuals, is increased to a detectable level, as observed in *Itpa*-KO mice. ITPA deficiency in patients with inflammatory bowel disease is, however, likely to be related to azathioprine intolerance, but does not cause any severe phenotype (19,20). To date, it is not known why ITPA deficiency causes a severe phenotype in mouse but not in humans. We, therefore, hypothesized that human cells are equipped with a compensatory mechanism which can efficiently suppress the ITPA deficiency.

In the present study, to identify novel ITP hydrolyzing enzymes or proteins that target ITP, we performed a comprehensive screen of proteins that specifically bind to ITP immobilized on Sepharose beads. We identified human nucleoside diphosphate linked moiety X-type motif 16 (NUDT16) protein (Swiss-Prot accession no., Q96DE0.2).

MATERIALS AND METHODS

Purification and identification of modified nucleotide-binding proteins

Modified nucleotide-binding proteins were purified and identified with pull-down assays as follows. γ-aminooctyl-nucleoside 5′-triphosphate-Sepharose (phosphate-NTP Sepharose) and/or 2′/3′-*O*-(2-aminoethylcarbamoyl)-nucleoside 5′-triphosphate-Sepharose (ribose-NTP Sepharose) for GTP, ATP, XTP, ITP, 8-oxo-GTP and 2-OH-ATP were purchased from Jena Bioscience (Jena, Germany) and used for pull-down assays. The cell extract of SH-SY5Y cells was prepared by sonication of cells in lysis buffer [1 ml for 5×10^7 cells, 25 mM Tris–HCl pH 7.5, 100 mM NaCl, 10 mM $MgCl_2$, 0.05% Nonidet P-40 (NP-40), 1 mM dithiothreitol (DTT), 1% protease inhibitor cocktail (Nacalai Tesque, Kyoto, Japan)] and clarified by centrifugation, as described previously (21). Protein concentration in the supernatant was measured with a DC-protein assay kit (Bio-Rad, Hercules, CA, USA) using bovine serum albumin (BSA) as a standard. Twenty microliters of each phosphate-NTP Sepharose, ribose-NTP Sepharose, and Sepharose carrier matrix were individually suspended in 1 ml of the supernatant, incubated for 15 min at 4°C, and washed three times with the lysis buffer without protease inhibitor cocktail. Bound proteins in each pulled-down sample were eluted with 40 μl of 2 × SDS sampling buffer (Sigma-Aldrich, St Louis, MO, USA), separated by SDS-PAGE, stained by silver staining with EzStain Silver kit (ATTO Co., Tokyo, Japan), and analyzed by LC-MS/MS, as described previously (21). Collision-induced dissociation spectra were acquired and compared with those in the International Protein Index (IPI version 3.26; European Bioinformatics Institute, Hinxton, UK) using the MASCOT search engine (Matrix Science, Boston, MA, USA). The high-scoring peptide sequences (MASCOT score >45) assigned by MASCOT were manually confirmed by comparison with the corresponding collision-induced dissociation spectra. Finally, we selected as candidate proteins those proteins for which multiple peptides were identified in this analysis.

Nucleotide-hydrolyzing assay with His-NUDT16

Each substrate nucleotide was incubated in reaction buffer (25 mM Tris–HCl pH 7.5, 150 mM KCl, 5 mM $MgCl_2$, 0.01% NP-40, 100 μg/ml BSA, 1 mM DTT) for 10 min at 37°C. Then, an equal volume of reaction buffer containing 100 μM recombinant NUDT16 with a His-tag at the N terminus (His-NUDT16), was mixed with the substrate solution. The mixture was further incubated at 37°C for 0–60 min, and then mixed with ice-cold EDTA to a final concentration of 50 mM to stop the reaction. The reaction products were clarified by centrifugation at 9000*g* for 5 min at 4°C, and then separated on a Wakopak Handy ODS column (Wako, Osaka, Japan) or on a TSK gel DEAE-2SW column (Tohso, Tokyo, Japan) using an HPLC system, at a flow rate of 0.6 ml/min with HPLC buffer 1 (0.1 M potassium phosphate buffer pH 4.0) or at 0.8 ml/min with HPLC buffer 2 (75 mM sodium phosphate buffer pH 6.4, 5% acetonitrile, 0.4 mM EDTA). Nucleotides were quantified by ultraviolet (UV) absorption. Kinetic parameters, k_{cat} and K_m, were calculated by a fit of the velocity data to the Michaelis–Menten equation using the SigmaPlot analysis software version 11 with Enzyme Kinetics Module 1.3 (Systat Software, San Jose, CA, USA).

Free phosphates were quantified colorimetrically with a modified Malachite Green phosphate detection method using Biomol Green reagent (Enzo Life Sciences International, Plymouth Meeting, PA, USA) (22,23). One-hundred microliters of the Biomol Green reagent was added to 50 μl of each reaction mixture, and the mixture was incubated for 30 min at room temperature. The change in absorbance at 620 nm was measured and used to determine free phosphate concentrations by comparison with a standard curve.

siRNA and transfection

All siRNA oligonucleotides used in this study, *NUDT16* siRNA#1 (*Silencer* Select *NUDT16* siRNA; #s43642), *NUDT16* siRNA#2 (*Silencer NUDT16* siRNA; #: 38731), control siRNA#1 (*Silencer* Select Negative Control #1 siRNA, Cat#4390844) and control siRNA#2 (*Silencer* Negative Control #1 siRNA, Cat#AM4635) were purchased from Applied Biosystems (Foster City, CA, USA). HeLa MR cells were transfected with siRNAs by electroporation using a Microporator-Mini (Digital Bio Technology, Seoul, Korea), according to the manufacturer's instructions. In brief, 10^5 cells were suspended in 10 µl of R buffer (provided in the MicroPoration kit) and mixed with 1 µl of one of the siRNAs (50 µM) before electroporation. The transfected cells were suspended in fresh culture medium. After incubation for 24 h, the cells were reseeded in new culture dishes at a density of $1.515 \times 10^3/cm^2$. After an additional incubation, the cells were subjected to further assays.

Immunofluorescence microscopy for NUDT16 and single-stranded DNA

To perform immunofluorescence microscopy for NUDT16 and single-stranded DNA (ssDNA), HeLa MR cells were seeded onto LaB-Tek two-well chamber slides (Thermo Fisher Scientific, Rockford, IL, USA), 24 h after transfection with control siRNA#1 or *NUDT16* siRNA#1. The cells were further cultured for 48 h and fixed with 4% paraformamide in phosphate buffered saline (PBS) containing 0.1% Triton X-100. The fixed cells were treated with anti-NUDT16 or with anti-nucleolin (sc-8031, Santa Cruz Biotechnology, Santa Cruz, CA, USA) in combination with Alexa Fluor 488-conjugated goat anti-rabbit IgG (A-11034, Invitrogen, Carlsbad, CA, USA) or Alexa Fluor 594-conjugated goat anti-mouse IgG (A-11032, Invitrogen). Nuclei were counterstained with 4′-diamino-2-phenylindole (DAPI) (50 ng/ml; Vector Laboratories, Burlingame, CA, USA). Digitized images were separately captured from identical fields using an LSM-510 Meta confocal microscopy system (Carl Zeiss, Oberkochen, Germany).

To detect ssDNA, slides were incubated with a 100 × dilution of anti-ssDNA (#18731, IBL, Takasaki, Japan) in combination with Alexa Fluor 488-conjugated goat anti-rabbit IgG. The anti-ssDNA antibody was raised against fragmented and denatured bovine DNA, and recognizes single stranded regions of DNA with a length of at least six deoxynucleotides length (24,25). Nuclei were counterstained with DAPI. The slide was observed under an Axioskop 2 plus, equipped with AxioCam and AxioVision software (Carl Zeiss). A total of 100 cells were examined for each preparation.

Quantification of deoxyinosine or inosine by LC-MS/MS

The DNA deoxyinosine or RNA inosine levels were determined as follows. The preparation and digestion of nuclear DNA samples were performed according to methods described previously (26), except that 10 mM 2, 2, 6, 6-tetramethylpiperidine-*N*-oxyl (TEMPO, Wako) and 20 µM 2′-deoxycoformycin, an adenosine deaminase inhibitor, kindly provided by the Chemo-Sero-Therapeutic Research Institute (Kumamoto, Japan), were added to all reagents at all stages of manipulation, according to the method described by Taghizadeh *et al.* (27). RNA was prepared using an RNeasy Mini Kit (Qiagen, Valencia, CA, USA) in the presence of 20 mM TEMPO and 20 µM 2′-deoxycoformycin. DNA or RNA samples were digested with Nuclease P1 (Yamasa, Chiba, Japan) and alkaline phosphatase (Sigma-Aldrich) in the presence of 20 mM TEMPO and 20 µM 2′-deoxycoformycin, and digested samples were subjected to LC-MS/MS analysis using the Shimadzu VP-10 HPLC system connected to the API3000 MS/MS system (PE-SCIEX), as described previously (26).

Cell cycle analysis

Flow cytometric analysis of the cell cycle was performed as previously described (28,29). Briefly, 1×10^6 cells were suspended in 1 ml PBS containing 0.2% Triton X for the naked nuclei preparation. Then, the cell suspension was passed through a nylon mesh membrane. Five microliters of RNase A (1 mg/ml) and 50 µl of propidium iodide (PI) (1 mg/ml) were then added to the suspension. DNA content and cell numbers were analyzed with an LSR flow cytometer (Becton Dickinson, San Jose, CA, USA). The data were analyzed with CellQuest and ModFit software (Becton Dickinson).

Karyotype analysis

Fifty-percent confluent cultures of HeLa MR cells were treated with 0.1 µg/ml colcemid (Nacalai Tesque) for 30 min and then harvested. After hypotonic treatment (75 mM KCl), cells were fixed in freshly prepared Carnoy's fixative (methanol:acetic acid; 3:1), and the cell suspension was dropped onto a glass slide, air-dried and immediately stained with freshly prepared Giemsa staining solution (Merck, 25 × diluted in PBS) for 20 min. After rinsing the slide twice in PBS and twice in distilled water, a cover slide was mounted onto the air-dried slide with Permount mounting medium (Thermo Fisher Scientific). The slide was observed under an Axio ImagerA.1 plus equipped with AxioCam and AxioVision software (Carl Zeiss). A total of 30 cells in metaphase were examined for each preparation.

Statistical analysis

All results are expressed as the mean ± SD. Statistical analysis was performed using Stat View 5.0 (SAS Institute, Cary, NC, USA) and each method of statistical analysis is shown in detail in the figure legends. $P < 0.05$ was considered statistically significant.

Supplementary materials and methods

Descriptions of the following materials and procedures are provided in Supplemental Experimental Procedures: free nucleotides, synthetic oligonucleotides, isolation of human *NUDT16* and mouse *Nudt16* cDNAs, construction of

expression plasmids, expression and purification of recombinant His-NUDT16 protein, anti-NUDT16, western blot analysis, cell culture, cell proliferation assay, Hoechst 33342/PI assay, real-time quantitative RT-PCR, and comet assay.

RESULTS

NUDT16 selectively binds to ITP, XTP and GTP

To search for ITP-binding proteins, we purified proteins from whole-cell extracts prepared from SH-SY5Y cells using a pull-down method incorporating various NTP-immobilized Sepharose beads (Figure 1A). The purified proteins were fractionated by SDS-PAGE and visualized by silver staining. The proteins in the gel were digested with trypsin and subjected to LC-MS/MS analysis (see 'Materials and Methods' section). By comparing retrieved proteins with multiple peptide sequences among all samples, we identified peptide fragments derived from NUDT16 only in the samples bound to phosphate/ribose-ITP, phosphate/ribose-XTP and ribose-GTP Sepharose beads, but not in samples bound to any other NTP Sepharose beads (Figure 1B and Supplementary Table S1). Western blot analysis of pull-down samples, prepared independently of the above samples using anti-NUDT16, confirmed the LC-MS/MS results by identifying the same nucleotide-binding 20 kDa NUDT16 protein (Figure 1C).

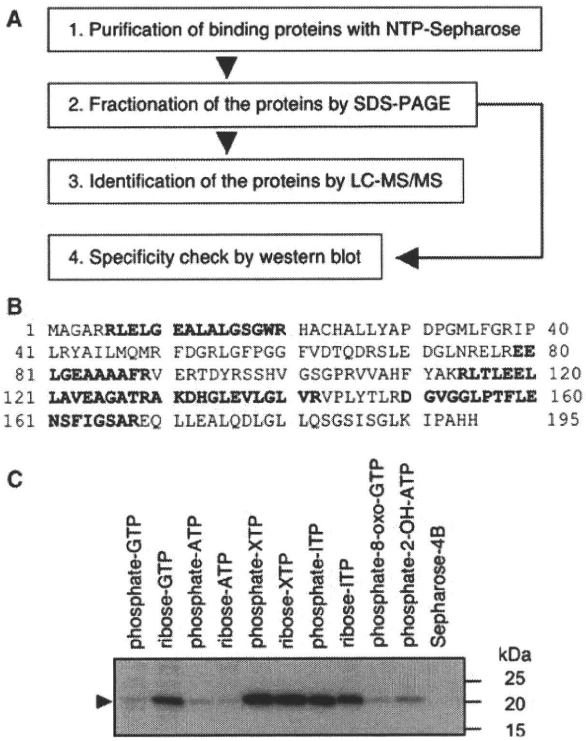

Figure 1. NUDT16 selectively binds to XTP, ITP and GTP. (**A**) Experimental scheme depicting the screen for nucleotide-binding proteins. Proteins in extracts prepared from SH-SY5Y cells were pulled down with NTP-immobilized Sepharose beads and subjected to SDS-PAGE, LC-MS/MS analysis and western blot analysis. (**B**) Amino acid sequence of NUDT16. Peptides detected by LC-MS/MS analysis in the screen are shown in bold (Mascot Ion Score >45). (**C**) Each sample, pulled down from the extract (219 μg total protein), was subjected to western blot analysis using anti-NUDT16 (lower panel). An arrowhead indicates signals for NUDT16.

NUDT16 is a (deoxy)inosine diphosphatase

Because NUDT16 is a member of the nudix family of proteins, including the nucleoside triphosphatase MTH1 (NUDT1), we performed biochemical analysis of nucleotide hydrolyzing activity using recombinant NUDT16 protein. His-NUDT16 was expressed in *Escherichia coli* (*E. coli*) and then purified. Samples from each purification step were subjected to SDS-PAGE and a His-NUDT16 polypeptide of ~23 kDa, (its calculated molecular weight is 23.45 kDa) was purified to near homogeneity after size exclusion column chromatography (Figure 2A).

When several canonical nucleotides were incubated with the purified His-NUDT16 protein, we found that His-NUDT16 effectively hydrolyzed IDP to IMP (Figure 2B, lower). We then determined the optimal conditions for the IDP hydrolysis by His-NUDT16. His-NUDT16 exhibited a temperature-dependent increase in its IDP hydrolyzing activity up to 60°C (Supplementary Figure S1A). IDP hydrolysis by His-NUDT16 gradually increased from pH 6.5 to 8.5 (Supplementary Figure S1B). IDP hydrolysis by His-NUDT16 was completely dependent on the presence of divalent cation, and increased linearly with increasing Mg^{2+} concentration up to 1 mM and then reached a plateau level (Supplementary Figure S1C). Zn^{2+} also increased His-NUDT16 activity in a dose-dependent manner, however, the activity observed in the presence of 10 mM Zn^{2+} was less than one-third of that observed in the presence of 1 mM Mg^{2+}. His-NUDT16 exhibited no IDP hydrolysis in the presence of 5 mM Mn^{2+}, Co^{2+} or Ca^{2+}. KCl, and to a lesser extent NaCl, moderately increased the activity in a dose-dependent manner up to 500 mM (Supplementary Figure S1D). Based on these results and in view of physiological conditions, we performed subsequent analyses of His-NUDT16 activity under the conditions of 25 mM Tris–HCl (pH 7.5), 5 mM Mg^{2+} and 150 mM KCl at 37°C.

To obtain an over view of substrate specificity for NUDT16, we incubated His-NUDT16 with various nucleotides at 10 or 100 μM (Figure 2C). The products were then analyzed and quantified by HPLC. His-NUDT16 hydrolyzed nucleoside triphosphates/diphosphates (NTPs/NDPs) to the corresponding nucleoside monophosphates (NMPs), and had substrate preferences for purine nucleotides. Especially at substrate concentrations of 10 μM, ITP, dITP, XDP, GDP, dGDP, IDP and dIDP were efficiently hydrolyzed. In contrast, His-NUDT16 did not generate any hydrolyzed product from 7-Me-GDP, ATP, CTP, UTP, 2-OH-ATP, dATP, dCTP, dUTP, TTP nor 2-OH-dATP, even at 100 μM. Because these substrates were not hydrolyzed, they are not represented in Figure 2C.

His-NUDT16 produced IMP from both ITP and IDP (Supplementary Figure S2 upper). To confirm the

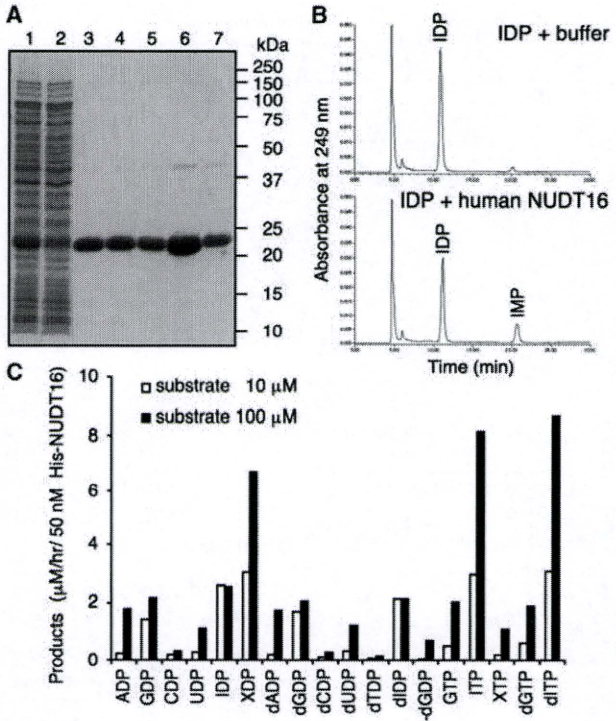

Figure 2. His-NUDT16 hydrolyzes (d)IDP in preference to other nucleotides. (**A**) Samples from the purification of recombinant His-NUDT16 were subjected to SDS-PAGE and GelCode Blue Staining. Lane 1, supernatant of *E. coli* extract; lane 2, flow-through fraction from the His-tag purification; lane 3, eluate from His-tag purification; lane 4, fraction recovered by ammonium sulfate precipitation; lane 5, sample after dialysis; lane 6, eluate from cation exchange chromatography; lane 7, fraction recovered from gel filtration chromatography. (**B**) IDP (200 μM) was incubated with 400 nM His-NUDT16 for 1 h at 37°C. Reaction products were analyzed by HPLC (lower panel), and were compared with substrate IDP incubated without His-NUDT16 (upper panel). HPLC chromatograms of both samples obtained by absorbance at 249 nm are shown. (**C**) Nucleoside di- or triphosphates (10 or 100 μM) were incubated with 50 nM His-NUDT16 for 1 h at 37°C. The reaction products were analyzed by HPLC. The graph shows the concentration of each nucleoside monophosphate product.

generation of free phosphates (Pi) in these reactions, we analyzed the products using the Malachite Green phosphate detection method to distinguish Pi from pyrophosphates (PPi). Hydrolysis of IDP by His-NUDT16 generated almost the same amounts of IMP and Pi; however, hydrolysis of ITP by His-NUDT16 generated IMP but not Pi (Supplementary Figure S2 lower). These results indicate that NUDT16 hydrolyzes IDP to IMP and Pi, while ITP is hydrolyzed to IMP and possibly PPi.

Because His-NUDT16 efficiently hydrolyzed ITP, dITP, XDP, GDP, dGDP, IDP and dIDP, we performed a detailed analysis of the hydrolysis kinetics for these substrates (Table 1). Fitting Michaelis–Menten type kinetics to the initial rates of reaction revealed a positive correlation for each substrate. Among the substrates, the k_{cat}/K_m values for IDP and dIDP were 251×10^3 and $183 \times 10^3\ s^{-1}\ M^{-1}$, respectively. These were at least seven times higher than the k_{cat}/K_m value for GDP ($26.2 \times 10^3\ s^{-1}\ M^{-1}$), which was the third highest among the substrates analyzed. IDP and dIDP were, therefore, identified as the best substrates for His-NUDT16.

Table 1. Kinetic parameters of His-NUDT16

Substrate	K_m μM	k_{cat} min^{-1}	k_{cat}/K_m $10^3\ s^{-1}\ M^{-1}$	Goodness-of-curve fit R^2
IDP	0.062	0.931	251	0.973
dIDP	0.088	0.966	183	0.990
GDP	0.330	0.518	26.1	0.987
dGDP	0.319	0.492	25.7	0.988
XDP	15.7	2.60	2.76	0.978
ITP	22.1	3.06	2.31	0.980
dITP	24.1	3.20	2.21	0.999

We also expressed mouse His-tagged NUDT16 protein (His-mNUDT16) in *E. coli* and analyzed dITP hydrolyzing activity using extracts prepared from *E. coli* cells with or without expression of His-mNUDT16. *E. coli* extract without His-mNUDT16 generated dIDP and dIMP from dITP. In contrast, *E. coli* extract with His-mNUDT16 generated only dIMP from dITP (Supplementary Figure S3). Thus, we concluded that mouse NUDT16 also hydrolyzes dIDP to dIMP.

Expression of NUDT16 in human cell lines and tissues

We determined the levels of *NUDT16* mRNA in 21 human tissues by real-time quantitative RT-PCR (Supplementary Figure S4). *NUDT16* mRNA was detected in all tissues examined and the highest expression was observed in lung and kidney. Next, we examined levels of *NUDT16* mRNA and protein in HeLa MR cells with or without (si)RNA silencing. Real-time quantitative RT-PCR revealed that *NUDT16* mRNA levels in HeLa MR cells were equivalent to those in heart and mammary gland. The introduction of *NUDT16* siRNA#1 significantly reduced the mRNA level to 17% of the control after 3 days (Figure 3A). Western blot analysis with anti-NUDT16 revealed a significantly reduced expression of a 20 kDa protein in HeLa MR cells, 2 and 4 days after the introduction of *NUDT16* siRNA#1 (Figure 3B). Other bands were consistently and uniformly detected in samples from cells treated with control siRNA#1 and *NUDT16* siRNA#1. The expression of the 20 kDa band partially recovered 7 days after the treatment, thus demonstrating that the 20 kDa protein is the endogenous NUDT16 protein of HeLa MR cells.

Next, we examined subcellular localization of NUDT16 protein in HeLa MR cells by immunofluorescence confocal laser scanning microscopy with anti-NUDT16 and anti-nucleolin, a nucleolar marker (Figure 3C). NUDT16 immunoreactivity was mostly detected in the DAPI-positive nuclei and partially detected in the cytoplasm (Figure 3C-a,b,d). The signal for NUDT16 was not uniformly localized in nuclei, but was intensely localized in a few small regions. The intense NUDT16 signals were mostly colocalized with the intense nucleolin signals where DAPI signals were faint (Figure 3C-d–f).

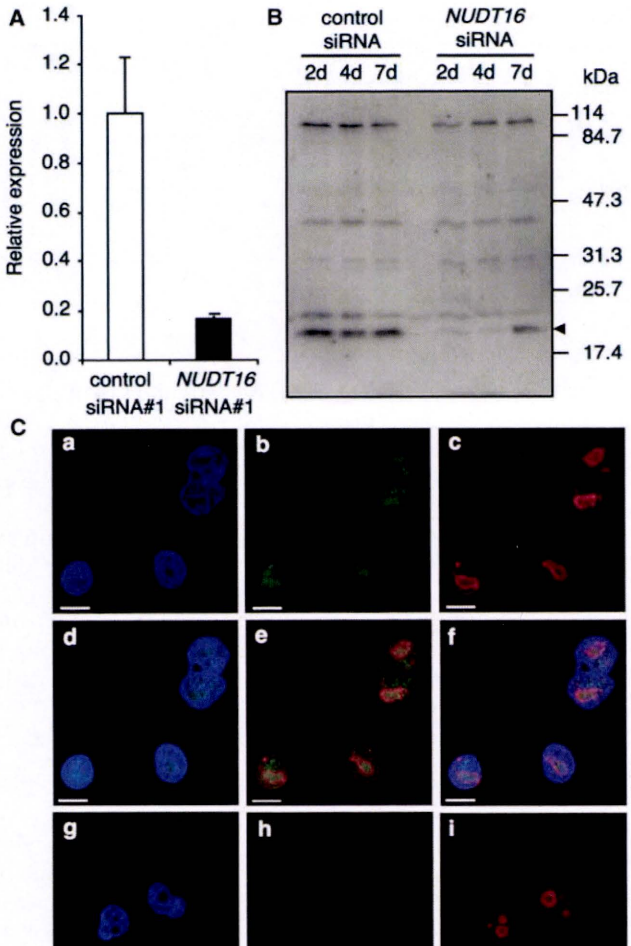

Figure 3. NUDT16 is mainly localized in nuclei, and especially in nucleoli. (**A**) Relative mRNA level after transfection of *NUDT16* siRNA. Three days after transfection with siRNAs, cells were harvested. The *NUDT16* mRNA level relative to that of the control was determined by real time quantitative RT-PCR and is shown as the mean ± SD of triplicate experiments. (**B**) Cells were transfected with siRNAs and harvested 2, 4, and 7 days after transfection. Cell extracts (10 μg total protein) were subjected to western blot analysis with anti-NUDT16. An arrowhead indicates signals for NUDT16. (**C**) Intracellular localization of NUDT16. HeLa MR cells were transfected with control siRNA#1 (a–f) or with *NUDT16* siRNA#1 (g–i). The cells were subjected to immunofluorescence microscopy with anti-NUDT16 (green, b and h) and anti-nucleolin (red, c and i). Nuclei were stained with DAPI (blue, a and g). Merged signals are shown in panel d (blue and green), e (green and red) and f (blue, green and red). Bars indicate 10 μm.

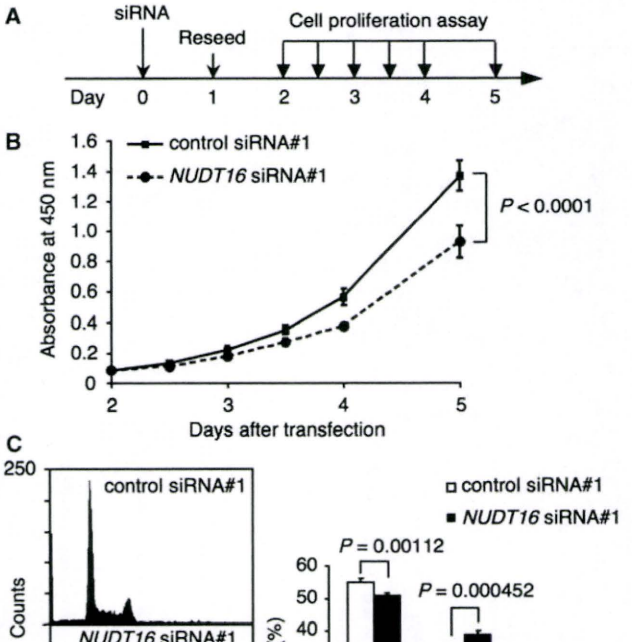

Figure 4. Knockdown of *NUDT16* suppresses proliferation of HeLa MR cells. (**A**) Experimental schedule. HeLa MR cells were transfected with siRNAs on Day 0. The transfected cells were then further incubated for 24 h before replating at a density of $1.5 \times 10^3/cm^2$. After an additional incubation, the cells were subjected to further analysis. (**B**) Cell proliferation assay. The cells in (A) were analyzed for cell proliferation. The graph shows the mean ± SD of results from three independent siRNA transfections. Two-way repeated measures ANOVA, $P < 0.0001$. (**C**) HeLa MR cells treated with *NUDT16* siRNA#1 show slightly abnormal progression of the cell cycle. Three days after siRNA transfection with *NUDT16* siRNA#1 or with control siRNA#1, cells were subjected to flow cytometry. Left panels indicate representative histograms of DNA contents in isolated nuclei from these cells. Data are mean ± SD of results from three independent siRNA transfections and were analyzed using Student's *t*-test.

Furthermore, most of the NUDT16 signals disappeared in cells treated with *NUDT16* siRNA#1 (Figure 3C-h). We thus concluded that NUDT16 protein is mostly localized in nucleoli.

Knockdown of NUDT16 expression suppresses proliferation of HeLa MR cells

To elucidate the biological functions of NUDT16, we examined the effects of *NUDT16* knockdown in HeLa MR cells. Twenty-four hours after the introduction of siRNA, the cells were reseeded. We then compared cell proliferation rates between cells treated with control siRNA#1 and those treated with *NUDT16* siRNA#1 (Figure 4A). *NUDT16* siRNA#1 significantly suppressed cell proliferation compared with the control siRNA (Figure 4B). Introduction of *NUDT16* siRNA#2, which has a different target sequence for *NUDT16*, also similarly suppressed the proliferation of HeLa MR cells, confirming the effect of *NUDT16* knockdown (Supplementary Figure S5A and B). Next, we performed a flow cytometric analysis of DNA content of HeLa MR cells after *NUDT16* knockdown. Cell cycle analysis revealed significantly increased S-phase and decreased G1 phase populations after introduction of *NUDT16* siRNA#1 (Figure 4C). Moreover, Hoechst 33342/PI

staining of the cells revealed that introduction of *NUDT16* siRNA#1 caused no obvious increase in the dead cell fraction (PI positive) in comparison to control siRNA#1 (Supplementary Figure S6). We observed no subG1 fraction, indicating that *NUDT16* knockdown did not induce cell death in our experimental conditions (Figure 4C).

Accumulation of inosine nucleotides in RNA and of single strand breaks in DNA after knockdown of NUDT16 expression

The localization of NUDT16 in nuclei strongly suggested that NUDT16 contributes to sanitization of the nuclear nucleotide pool, which supplies precursors for the synthesis of RNA and DNA. We, therefore, measured inosine in cellular RNA and deoxyinosine in nuclear DNA in HeLa MR cells after *NUDT16* knockdown by siRNA. The inosine level in RNA was significantly increased in cells treated with *NUDT16* siRNA#1 (36.1 ± 1.35 inosine residues per 10^6 guanosine residues) compared with cells treated with control siRNA#1 (31.9 ± 1.05 inosine residues per 10^6 guanosine residues) ($P = 0.0125$) (Figure 5A right). However, there was no significant difference in the deoxyinosine level in DNA between the two conditions (Figure 5A left). These results suggested that ITP or dITP levels are increased after *NUDT16* knockdown, and that their incorporation into RNA or DNA may be similarly increased; however, deoxyinosine incorporated into newly synthesized DNA might be quickly eliminated by DNA repair enzymes. DNA repair processes often form ssDNA regions as repair intermediates (30–32). Therefore, we examined ssDNA accumulation in nuclear DNA of HeLa MR cells by immunofluorescence detection using an anti-ssDNA antibody after siRNA treatment. The anti-ssDNA antibody was raised against fragmented bovine DNA, and recognizes ssDNA generated by double- or single-strand DNA breaks (33). Following treatment with *NUDT16* siRNA, the percentage of ssDNA-positive HeLa MR cells (13.9%) was 5.3 times higher than that treated with control siRNA ($P = 0.000252$) (Figure 5B). ssDNA regions can be generated by either single- or double-strand breaks in DNA. In the comet assay, HeLa

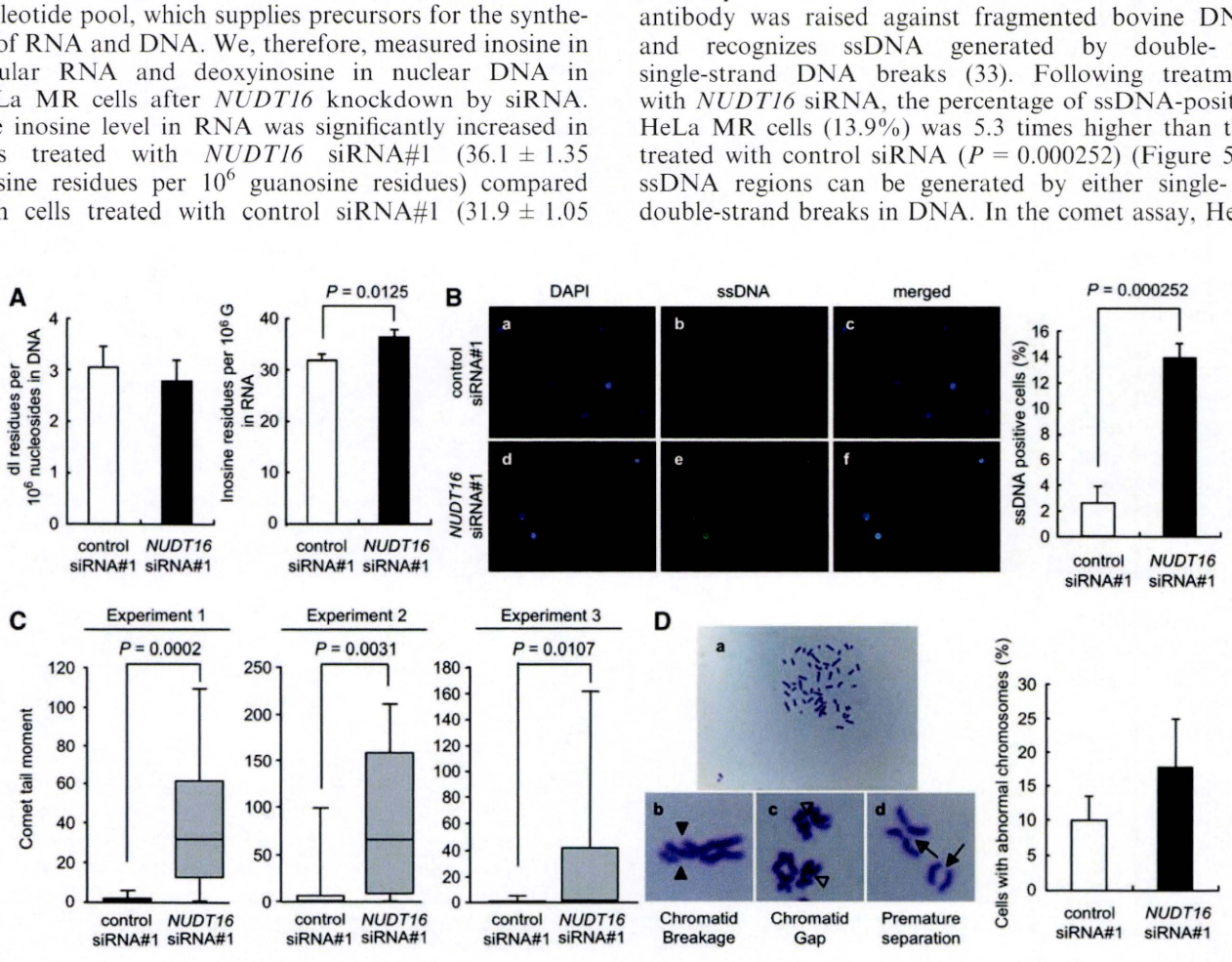

Figure 5. Knockdown of *NUDT16* in HeLa MR cells increases the number of inosine residues in RNA and the level of single strand breaks in nuclear DNA. HeLa MR cells were independently transfected with siRNAs three times. Three days after transfection, cells were subjected to the following analysis. (**A**) Quantification of inosine or deoxyinosine by LC-MS/MS. HeLa MR cells were harvested to determine the levels of inosine and deoxyinosine [dI]. The numbers of deoxyinosine residues [dI] per 10^6 nucleosides in DNA or inosine residues per 10^6 guanosine [G] in RNA from three independent transfections are shown. Student's *t*-test, $P = 0.0125$ (RNA). (**B**) Knockdown of *NUDT16* induces the accumulation of ssDNA in nuclei of HeLa MR cells. HeLa MR cells transfected with control siRNA#1 (a–c) or with *NUDT16* siRNA#1 (d–f) were subjected to immunofluorescence microscopy with anti-ssDNA (green, b and e). Nuclei were stained with DAPI (blue, a and d). Merged signals are shown in c and f (blue and green). Percentages of ssDNA-positive nuclei among DAPI-positive nuclei are shown in the bar graph. Data are mean ± SD of three independent siRNA transfections. Student's *t*-test, $P = 0.000252$. (**C**) Comet assay under alkaline conditions. Tail moments of at least 15 cells were calculated for each group and box-and-whisker plots are shown for three independent assays. Mann–Whitney U-test, $P < 0.05$. (**D**) Chromosomal abnormality. Transfected cells were prepared as in (B). Mitotic cells with chromosomal abnormalities (a) were defined as cells with chromatid breakage (b; solid arrowheads), chromatid gap (c; open arrowheads) and/or premature separation (d; arrows). These cells were counted and percentages of cells with chromosomal abnormalities among thirty mitotic cells are shown in the bar graph. Chromatid breakage, chromatid gap, and premature separation in control cells were 8%, 2% and 0%, respectively, and in *NUDT16* knockdown cells were12%, 4% and 1%, respectively. Data are mean ± SD from three independent siRNA transfections.

MR cells transfected with *NUDT16* siRNA showed a significantly increased tail moment under alkaline conditions in three independent experiments ($P < 0.05$, Mann–Whitney U-test), but not under neutral conditions (Figure 5C and Supplementary Figure S7). Cells exposed to hydrogen peroxide, which is known to cause double-strand breaks, exhibited a significantly increased tail moment, even under neutral conditions; therefore we concluded that knockdown of *NUDT16* caused accumulation of single-strand breaks in nuclear DNA. Next, chromosome abnormalities including chromatid breakage, chromatid gap, and/or premature separation were examined in mitotic cells. The percentage of the cells with abnormal chromosomes in HeLa MR cells treated with *NUDT16* siRNA was 1.8 times higher than that in cells treated with control siRNA, although the difference was not significant ($P = 0.115$) (Figure 5D).

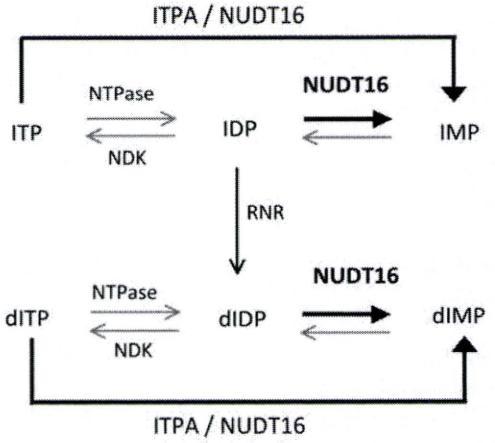

Figure 6. Model of biological roles of NUDT16. NUDT16 eliminates (d)IDP and (d)ITP from the nucleotide pools in cooperation with ITPA. NDK; nucleoside diphosphate kinases, RNR; ribonucleotide reductase.

DISCUSSION

In the present study, we reported two major findings; first, NUDT16 hydrolyzes (d)IDP/(d)ITP and second, NUDT16 deficiency induces accumulation of single strand breaks in nuclear DNA and growth arrest in human cells.

Previously, Ghosh *et al.* (34) reported that NUDT16 recognizes the 5′-cap structure of U8 small nucleolar RNA (snoRNA) and weakly hydrolyzes it to produce non-capped-snoRNA with guanosine 5′-monophosphate at its 5′-terminus and an excised cap. First guanosine residue of U8 snoRNA itself is linked to the triphosphate following the 5′-cap, and thus mimicking a GTP structure. GTP was shown to be weakly hydrolyzed by NUDT16 in the present study. Therefore, both 5′-capped U8 snoRNA and GTP can be converted by NUDT16 to guanosine 5′-monophosphate (GMP) at the 5′-terminal end of snoRNA and to free GMP, respectively. Thus, it is likely that hydrolysis of GTP and decapping of U8 snoRNA are essentially the same enzyme reaction of NUDT16. We also showed that in a human cell line, NUDT16 is localized in nuclei, mainly nucleoli. Similarly, Ghosh *et al.* (34) have reported that X29 protein, the *Xenopus* homolog of NUDT16, is primarily a nucleolar protein in *Xenopus* cells *in vitro*.

As shown in Figure 6, NUDT16 efficiently hydrolyzes (d)IDP, and hydrolyzes (d)ITP to a lesser extent. (d)ITP and (d)IDP can be generated by deamination of adenine nucleotides or phosphorylation of (d)IMP (35). ITPA, which is relatively abundant in the cytoplasm and which is encoded by *ITPA*, is known to hydrolyze (d)ITP to (d)IMP and pyrophosphate (14,15). The study of NUDT16 reaction kinetics revealed that NUDT16 has a lower hydrolysis rate but a higher affinity for (d)ITP compared with ITPA (for ITP; NUDT16, k_{cat} 3.2 min^{-1}, K_m 22.1 μM; ITPA, k_{cat} 34 800 min^{-1}, K_m 510 μM) (15). NUDT16, therefore, might be an important enzyme for the elimination of (deoxy)inosine nucleotides from nuclei, especially at low concentrations. Because NUDT16 is localized mainly in nucleoli, NUDT16 may prevent the incorporation of inosine nucleotides into ribosomal RNA (rRNA) during transcription. An increase in the RNA inosine level, observed after the knockdown of *NUDT16* supports this hypothesis. NUDT16, but not ITPA, has a strong hydrolysis activity for (d)IDP. In the pathway converting abundant cellular IMP to ITP by phosphorylation (10), IDP is an important intermediate. In addition, IDP is expected to be converted to dIDP by ribonucleotide reductase (36), and dIDP can be phosphorylated, thereby resulting in increased levels of dITP (11).

8-oxo-dGTP is known to be incorporated into genomic DNA and to induce mutation in both mammalian and bacterial cells (3). Human NUDT5, which hydrolyzes 8-oxo-dGDP, was reported to decrease spontaneous mutation in *E. coli mutT*$^-$ cells deficient in 8-oxo-dGTP hydrolyzing activity (37). Taken together with our findings on NUDT16, these results support the importance of the elimination of modified (deoxy)nucleoside diphosphates from the nucleotide pools.

In the present study, we observed the deoxyinosine levels in nuclear DNA within the normal ranges previously observed by Taghizadeh *et al.* (27) even after knockdown of *NUDT16*. However, knockdown of *NUDT16* expression increased the fraction of ssDNA-positive cells. We assume that the dITP level in the nuclear nucleotide pool must increase after *NUDT16* knockdown, thus resulting in increased incorporation of deoxyinosine into newly synthesized DNA. The deoxyinosine in DNA is immediately removed by the DNA repair process, resulting in an accumulation of ssDNA. Bradshaw and Kuzminov (38) described the incorporation of dITP/dXTP into the genomic DNA of *rdgB*$^-$ *E. coli* cells, which lack bacterial ITPase. In *E. coli* cells, DNA containing deoxyinosine can be excised by Endo V-initiated nucleotide excision repair, thus resulting in DNA strand breakage (32). Both Endo V and another enzyme, alkyl-adenine-DNA glycosylase (AAG, MAG, ANPG, MPG) were reported as candidates for hypoxanthine specific DNA repair enzymes in

mammalian cells (39–41). It is well known that increased accumulation of ssDNA triggers the DNA damage response, to induce delay in S-phase, and then cell cycle arrest (42). We, therefore, assume that the DNA damage response, to the accumulation of ssDNA, suppresses cell cycle progression, thus increasing the S-phase population and resulting in a decreased proliferation rate. On the other hand, knockdown of NUDT16 expression induced a 13.3% increase in RNA inosine levels. RNA editing by adenosine deaminases is a well-known system of post-transcriptional regulation and the major source of inosine in RNA; therefore, more inosine residues are present in RNA compared with deoxyinosine residues in DNA (43,44). Inosine, produced in RNA by such a regulated system, is thought to cause important modifications to the functions of non-coding RNA, or to alter amino acid sequence encoded by mRNA (45,46). In other words, unregulated incorporation of inosine during RNA transcription might impair RNA functions. In the present study, we demonstrated that NUDT16 contributes to the suppression of such inosine incorporation into RNA. Although the increased level of inosine in RNA under NUDT16 deficiency was statistically significant and the net increase was much higher than the basal level of deoxyinosine in DNA (4.3 inosine/10^6 G versus 0.63 deoxyinosine/10^6 dG), the higher basal level of inosine in RNA (32 inosine/10^6 G), which is likely to be generated by RNA-editing (45,46), made the difference appear small.

We previously reported that *Itpa*$^{-/-}$ mice showed growth retardation and heart failure and did not survive beyond 2 weeks after birth (16). Following this report, we found that primary mouse embryonic fibroblasts (MEFs) prepared from *Itpa*$^{-/-}$ mice showed a significantly prolonged doubling time and chromosomal abnormalities, accompanied by increased ssDNA and deoxyinosine residues in nuclear DNA (47). However, once *Itpa*$^{-/-}$ MEFs were spontaneously immortalized, the immortalized *Itpa*$^{-/-}$ MEFs had neither of these phenotypes. Furthermore, immortalized *Itpa*$^{-/-}$ MEFs exhibited significantly increased levels of *Nudt16* mRNA and protein. siRNA-mediated knockdown of *Nudt16* in immortalized *Itpa*$^{-/-}$ MEFs significantly increased deoxyinosine levels in nuclear DNA, and thus reproduced the ITPA-deficient phenotype. We, therefore, concluded that mouse NUDT16 functions as a backup enzyme for the ITPA deficiency by eliminating (d)IDP, and to a lesser extent (d)ITP from the nucleotide pools in MEFs. In wild-type MEFs, knockdown of *Nudt16* did not result in such phenotypes, indicating that mouse ITPA can compensate for the deficiency of NUDT16 in MEFs. In contrast, our present data suggested that human ITPA itself cannot completely compensate for the deficiency of NUDT16 in HeLa MR cells, although double deficiency of ITPA and NUDT16 would cause more severe phenotypes. Human individuals with ITPA deficiency show no obvious phenotypes. Thus, ITPA deficiency causes quite different effects in mouse and human. Comparing the expression level or enzyme activity of NUDT16 between mouse and human might explain why human cells have a significant tolerance to ITPA deficiency. In the present study, partial reduction of *NUDT16* expression in HeLa MR cells was sufficient to cause growth suppression and accumulation of single-strand breaks in nuclear DNA. Therefore, defective NUDT16 might lead to genome-instability syndromes in human individuals.

SUPPLEMENTARY DATA

Supplementary Data are available at NAR Online.

ACKNOWLEDGEMENTS

We thank Drs M. Matsumoto and K. Oyamada, from the Division of Cell Biology of the Medical Institute of Bioregulation, for helpful discussions. We thank M. Oda, E. Koba and M. Ohtsu, from the Laboratory for Technical Support of the Medical Institute of Bioregulation, and N. Adachi and K. Asakawa for their technical assistance.

FUNDING

The Ministry of Education, Culture, Sports, Science and Technology of Japan (20013034 to Y.N., 21117512 to D.T.); Japan Society for the Promotion of Science (19390114 to D.T., 08J03650 to T.I.); Kyushu University Global COE program (to Y.N.). Funding for open access charge: The Ministry of Education, Culture, Sports, Science and Technology of Japan (21117512 to D.T.).

Conflict of interest statement. None declared.

REFERENCES

1. Friedberg,E.C., Walker,G.C., Siede,W., Wood,R.D., Schultz,R.A. and Ellenberger,T. (2005) *DNA Repair And Mutagenesis*, 2nd edn. ASM Press, Washington.
2. Nakabeppu,Y., Sakumi,K., Sakamoto,K., Tsuchimoto,D., Tsuzuki,T. and Nakatsu,Y. (2006) Mutagenesis and carcinogenesis caused by the oxidation of nucleic acids. *Biol. Chem.*, **387**, 373–379.
3. Tsuzuki,T., Nakatsu,Y. and Nakabeppu,Y. (2007) Significance of error-avoiding mechanisms for oxidative DNA damage in carcinogenesis. *Cancer Sci.*, **98**, 465–470.
4. Nakabeppu,Y., Kajitani,K., Sakamoto,K., Yamaguchi,H. and Tsuchimoto,D. (2006) MTH1, an oxidized purine nucleoside triphosphatase, prevents the cytotoxicity and neurotoxicity of oxidized purine nucleotides. *DNA Repair*, **5**, 761–772.
5. Nakabeppu,Y., Tsuchimoto,D., Yamaguchi,H. and Sakumi,K. (2007) Oxidative damage in nucleic acids and Parkinson's disease. *J. Neurosci. Res.*, **85**, 919–934.
6. Rai,P., Onder,T.T., Young,J.J., McFaline,J.L., Pang,B., Dedon,P.C. and Weinberg,R.A. (2009) Continuous elimination of oxidized nucleotides is necessary to prevent rapid onset of cellular senescence. *Proc. Natl Acad. Sci. USA*, **106**, 169–174.
7. el-Hajj,H.H., Zhang,H. and Weiss,B. (1988) Lethality of a *dut* (deoxyuridine triphosphatase) mutation in *Escherichia coli*. *J. Bacteriol.*, **170**, 1069–1075.
8. Nguyen,T., Brunson,D., Crespi,C.L., Penman,B.W., Wishnok,J.S. and Tannenbaum,S.R. (1992) DNA damage and mutation in human cells exposed to nitric oxide in vitro. *Proc. Natl Acad. Sci. USA*, **89**, 3030–3034.
9. Traut,T.W. (1994) Physiological concentrations of purines and pyrimidines. *Mol. Cell. Biochem.*, **140**, 1–22.
10. Vanderheiden,B.S. (1979) Inosine di- and triphosphate synthesis in erythrocytes and cell extracts. *J. Cell. Physiol.*, **99**, 287–301.

11. Myrnes,B., Guddal,P.H. and Krokan,H. (1982) Metabolism of dITP in HeLa cell extracts, incorporation into DNA by isolated nuclei and release of hypoxanthine from DNA by a hypoxanthine-DNA glycosylase activity. *Nucleic Acids Res.*, **10**, 3693–3701.
12. Schouten,K.A. and Weiss,B. (1999) Endonuclease V protects *Escherichia coli* against specific mutations caused by nitrous acid. *Mutat. Res.*, **435**, 245–254.
13. Yasui,M., Suenaga,E., Koyama,N., Masutani,C., Hanaoka,F., Gruz,P., Shibutani,S., Nohmi,T., Hayashi,M. and Honma,M. (2008) Miscoding properties of 2′-deoxyinosine, a nitric oxide-derived DNA Adduct, during translesion synthesis catalyzed by human DNA polymerases. *J. Mol. Biol.*, **377**, 1015–1023.
14. Behmanesh,M., Sakumi,K., Tsuchimoto,D., Torisu,K., Ohnishi-Honda,Y., Rancourt,D.E. and Nakabeppu,Y. (2005) Characterization of the structure and expression of mouse *Itpa* gene and its related sequences in the mouse genome. *DNA Res.*, **12**, 39–51.
15. Lin,S., McLennan,A.G., Ying,K., Wang,Z., Gu,S., Jin,H., Wu,C., Liu,W., Yuan,Y., Tang,R. *et al.* (2001) Cloning, expression, and characterization of a human inosine triphosphate pyrophosphatase encoded by the *ITPA* gene. *J. Biol. Chem.*, **276**, 18695–18701.
16. Behmanesh,M., Sakumi,K., Abolhassani,N., Toyokuni,S., Oka,S., Ohnishi,Y.N., Tsuchimoto,D. and Nakabeppu,Y. (2009) ITPase-deficient mice show growth retardation and die before weaning. *Cell Death Differ.*, **16**, 1315–1322.
17. Burton,K., White,H. and Sleep,J. (2005) Kinetics of muscle contraction and actomyosin NTP hydrolysis from rabbit using a series of metal-nucleotide substrates. *J. Physiol.*, **563**, 689–711.
18. Maeda,T., Sumi,S., Ueta,A., Ohkubo,Y., Ito,T., Marinaki,A.M., Kurono,Y., Hasegawa,S. and Togari,H. (2005) Genetic basis of inosine triphosphate pyrophosphohydrolase deficiency in the Japanese population. *Mol. Genet. Metab.*, **85**, 271–279.
19. Sumi,S., Marinaki,A.M., Arenas,M., Fairbanks,L., Shobowale-Bakre,M., Rees,D.C., Thein,S.L., Ansari,A., Sanderson,J., De Abreu,R.A. *et al.* (2002) Genetic basis of inosine triphosphate pyrophosphohydrolase deficiency. *Hum. Genet.*, **111**, 360–367.
20. Marinaki,A.M., Duley,J.A., Arenas,M., Ansari,A., Sumi,S., Lewis,C.M., Shobowale-Bakre,M., Fairbanks,L.D. and Sanderson,J. (2004) Mutation in the *ITPA* gene predicts intolerance to azathioprine. *Nucleosides Nucleotides Nucleic Acids*, **23**, 1393–1397.
21. Nonaka,M., Tsuchimoto,D., Sakumi,K. and Nakabeppu,Y. (2009) Mouse RS21-C6 is a mammalian 2′-deoxycytidine 5′-triphosphate pyrophosphohydrolase that prefers 5-iodocytosine. *FEBS J.*, **276**, 1654–1666.
22. Klaus,S.M., Wegkamp,A., Sybesma,W., Hugenholtz,J., Gregory,J.F.III. and Hanson,A.D. (2005) A nudix enzyme removes pyrophosphate from dihydroneopterin triphosphate in the folate synthesis pathway of bacteria and plants. *J. Biol. Chem.*, **280**, 5274–5280.
23. Xu,W., Shen,J., Dunn,C.A., Desai,S. and Bessman,M.J. (2001) The Nudix hydrolases of *Deinococcus radiodurans*. *Mol. Microbiol.*, **39**, 286–290.
24. Oka,S., Ohno,M., Tsuchimoto,D., Sakumi,K., Furuichi,M. and Nakabeppu,Y. (2008) Two distinct pathways of cell death triggered by oxidative damage to nuclear and mitochondrial DNAs. *EMBO J.*, **27**, 421–432.
25. Kawarada,Y., Miura,N. and Sugiyama,T. (1998) Antibody against single-stranded DNA useful for detecting apoptotic cells recognizes hexadeoxynucleotides with various base sequences. *J. Biochem.*, **123**, 492–498.
26. Tsuruya,K., Furuichi,M., Tominaga,Y., Shinozaki,M., Tokumoto,M., Yoshimitsu,T., Fukuda,K., Kanai,H., Hirakata,H., Iida,M. *et al.* (2003) Accumulation of 8-oxoguanine in the cellular DNA and the alteration of the OGG1 expression during ischemia-reperfusion injury in the rat kidney. *DNA Repair*, **2**, 211–229.
27. Taghizadeh,K., McFaline,J.L., Pang,B., Sullivan,M., Dong,M., Plummer,E. and Dedon,P.C. (2008) Quantification of DNA damage products resulting from deamination, oxidation and reaction with products of lipid peroxidation by liquid chromatography isotope dilution tandem mass spectrometry. *Nat. Protoc.*, **3**, 1287–1298.
28. Yamazaki,K., Guo,L., Sugahara,K., Zhang,C., Enzan,H., Nakabeppu,Y., Kitajima,S. and Aso,T. (2002) Identification and biochemical characterization of a novel transcription elongation factor, Elongin A3. *J. Biol. Chem.*, **277**, 26444–26451.
29. Ide,Y., Tsuchimoto,D., Tominaga,Y., Nakashima,M., Watanabe,T., Sakumi,K., Ohno,M. and Nakabeppu,Y. (2004) Growth retardation and dyslymphopoiesis accompanied by G2/M arrest in APEX2-null mice. *Blood*, **104**, 4097–4103.
30. Hegde,M.L., Hazra,T.K. and Mitra,S. (2008) Early steps in the DNA base excision/single-strand interruption repair pathway in mammalian cells. *Cell Res.*, **18**, 27–47.
31. Demple,B. and DeMott,M.S. (2002) Dynamics and diversions in base excision DNA repair of oxidized abasic lesions. *Oncogene*, **21**, 8926–8934.
32. Weiss,B. (2008) Removal of deoxyinosine from the *Escherichia coli* chromosome as studied by oligonucleotide transformation. *DNA Repair*, **7**, 205–212.
33. Naruse,I., Keino,H. and Kawarada,Y. (1994) Antibody against single-stranded DNA detects both programmed cell death and drug-induced apoptosis. *Histochemistry*, **101**, 73–78.
34. Ghosh,T., Peterson,B., Tomasevic,N. and Peculis,B.A. (2004) *Xenopus* U8 snoRNA binding protein is a conserved nuclear decapping enzyme. *Mol. Cell*, **13**, 817–828.
35. Shenoy,T.S. and Clifford,A.J. (1975) Adenine nucleotide metabolism in relation to purine enzymes in liver, erythrocytes and cultured fibroblasts. *Biochim. Biophys. Acta*, **411**, 133–143.
36. Burgis,N.E. and Cunningham,R.P. (2007) Substrate specificity of RdgB protein, a deoxyribonucleoside triphosphate pyrophosphohydrolase. *J. Biol. Chem.*, **282**, 3531–3538.
37. Ishibashi,T., Hayakawa,H. and Sekiguchi,M. (2003) A novel mechanism for preventing mutations caused by oxidation of guanine nucleotides. *EMBO Rep.*, **4**, 479–483.
38. Bradshaw,J.S. and Kuzminov,A. (2003) RdgB acts to avoid chromosome fragmentation in *Escherichia coli*. *Mol. Microbiol.*, **48**, 1711–1725.
39. Moe,A., Ringvoll,J., Nordstrand,L.M., Eide,L., Bjoras,M., Seeberg,E., Rognes,T. and Klungland,A. (2003) Incision at hypoxanthine residues in DNA by a mammalian homologue of the *Escherichia coli* antimutator enzyme endonuclease V. *Nucleic Acids Res.*, **31**, 3893–3900.
40. Lee,C.Y., Delaney,J.C., Kartalou,M., Lingaraju,G.M., Maor-Shoshani,A., Essigmann,J.M. and Samson,L.D. (2009) Recognition and processing of a new repertoire of DNA substrates by human 3-methyladenine DNA glycosylase (AAG). *Biochemistry*, **48**, 1850–1861.
41. Saparbaev,M., Mani,J.C. and Laval,J. (2000) Interactions of the human, rat, *Saccharomyces cerevisiae* and *Escherichia coli* 3-methyladenine-DNA glycosylases with DNA containing dIMP residues. *Nucleic Acids Res.*, **28**, 1332–1339.
42. Lazzaro,F., Giannattasio,M., Puddu,F., Granata,M., Pellicioli,A., Plevani,P. and Muzi-Falconi,M. (2009) Checkpoint mechanisms at the intersection between DNA damage and repair. *DNA Repair*, **8**, 1055–1067.
43. Athanasiadis,A., Rich,A. and Maas,S. (2004) Widespread A-to-I RNA editing of Alu-containing mRNAs in the human transcriptome. *PLoS Biol.*, **2**, e391.
44. Paul,M.S. and Bass,B.L. (1998) Inosine exists in mRNA at tissue-specific levels and is most abundant in brain mRNA. *EMBO J.*, **17**, 1120–1127.
45. Nishikura,K. (2006) Editor meets silencer: crosstalk between RNA editing and RNA interference. *Nat. Rev. Mol. Cell. Biol.*, **7**, 919–931.
46. Schaub,M. and Keller,W. (2002) RNA editing by adenosine deaminases generates RNA and protein diversity. *Biochimie*, **84**, 791–803.
47. Abolhassani,N., Iyama,T., Tsuchimoto,D., Sakumi,K., Ohno,M., Behmanesh,M. and Nakabeppu,Y. (2010) NUDT16 and ITPA play a dual protective role in maintaining chromosome stability and cell growth by eliminating dIDP/IDP and dITP/ITP from nucleotide pools in mammals. *Nucleic Acids Res.*, doi:10.1093/nar/gkp1250.

Published online 15 January 2010

Nucleic Acids Research, 2010, Vol. 38, No. 9 ***2891–2903***
doi:10.1093/nar/gkp1250

NUDT16 and ITPA play a dual protective role in maintaining chromosome stability and cell growth by eliminating dIDP/IDP and dITP/ITP from nucleotide pools in mammals

Nona Abolhassani, Teruaki Iyama, Daisuke Tsuchimoto, Kunihiko Sakumi, Mizuki Ohno, Mehrdad Behmanesh and Yusaku Nakabeppu*

Division of Neurofunctional Genomics, Department of Immunobiology and Neuroscience, Medical Institute of Bioregulation, Kyushu University, Fukuoka, 812-8582, Japan

Received November 28, 2009; Revised December 20, 2009; Accepted December 26, 2009

ABSTRACT

Mammalian inosine triphosphatase encoded by *ITPA* gene hydrolyzes ITP and dITP to monophosphates, avoiding their deleterious effects. *Itpa*$^{-}$ mice exhibited perinatal lethality, and significantly higher levels of inosine in cellular RNA and deoxyinosine in nuclear DNA were detected in *Itpa*$^{-}$ embryos than in wild-type embryos. Therefore, we examined the effects of ITPA deficiency on mouse embryonic fibroblasts (MEFs). *Itpa*$^{-}$ primary MEFs lacking ITP-hydrolyzing activity exhibited a prolonged doubling time, increased chromosome abnormalities and accumulation of single-strand breaks in nuclear DNA, compared with primary MEFs prepared from wild-type embryos. However, immortalized *Itpa*$^{-}$ MEFs had neither of these phenotypes and had a significantly higher ITP/IDP-hydrolyzing activity than *Itpa*$^{-}$ embryos or primary MEFs. Mammalian NUDT16 proteins exhibit strong dIDP/IDP-hydrolyzing activity and similarly low levels of *Nudt16* mRNA and protein were detected in primary MEFs derived from both wild-type and *Itpa*$^{-}$ embryos. However, immortalized *Itpa*$^{-}$ MEFs expressed significantly higher levels of *Nudt16* than the wild type. Moreover, introduction of silencing RNAs against *Nudt16* into immortalized *Itpa*$^{-}$ MEFs reproduced ITPA-deficient phenotypes. We thus conclude that NUDT16 and ITPA play a dual protective role for eliminating dIDP/IDP and dITP/ITP from nucleotide pools in mammals.

INTRODUCTION

The accumulation of modified or damaged bases in genomic DNA is a major threat for the alteration of genetic information as a result of mutagenesis or even for programmed cell death. It has been established that such damaged bases in genomic DNA arise from two independent pathways: one is a consequence of the direct modification of the normal bases in the DNA and the other is that of the incorporation of modified nucleotides generated in resident nucleotide pools (1,2).

To control the quality of the nucleotide pools, organisms possess a number of nucleoside triphosphatases, which degrade non-canonical nucleoside triphosphates to the corresponding monophosphates. We had identified and characterized three mammalian enzymes: (i) oxidized purine nucleoside triphosphatase encoded by *MTH1* gene for 8-oxo-2′-deoxyguanosine triphosphate (8-oxo-dGTP), 8-oxoGTP, 2-hydroxy-2′-deoxyadenosine triphosphate (2-OH-dATP) and 2-OH-ATP (3,4); (ii) inosine triphosphatase encoded by *ITPA* gene for deaminated purine nucleoside triphosphates such as 2′-deoxyinosine triphosphate (dITP), ITP and 2′-deoxyxanthosine triphosphate (dXTP) and XTP (5,6); and (iii) a newly discovered enzyme, dCTP pyrophosphatase encoded by *DCTPP1* gene for halogenated dCTPs such as 5-iodo-2′-deoxycytidine triphosphate (7).

To clarify the biological significance of the damaged nucleotides and the enzymes that eliminate them, we had

*To whom correspondence should be addressed. Tel: +81 92 642 6800; Fax: +81 92 642 6791; Email: yusaku@bioreg.kyushu-u.ac.jp
Correspondence may also be addressed to Daisuke Tsuchimoto. Tel: +81 92 642 6802; Fax: +81 92 642 6804;
Email: daisuke@bioreg.kyushu-u.ac.jp
Present addresses:
Mizuki Ohno, Department of Medical Biophysics and Radiation Biology, Faculty of Medical Sciences, Kyushu University, Fukuoka 812-8582, Japan
Mehrdad Behmanesh, Department of Genetics, School of Biological Sciences, Tarbiat Modares University, Tehran, 14115-175, Iran